A Review of the Impact of Blue Space on the Urban Microclimate

P. Ampatzidis & T. Kershaw

Department of Architecture and Civil Engineering,

University of Bath,

Claverton Down, Bath

BA2 7AY, UK

Corresponding author: t.j.kershaw@bath.ac.uk

Keywords: heat island, climate, waterbody, blue space, cooling, microclimate.

Abstract

The urban heat island (UHI) phenomenon represents a major public health issue and has received great attention due to rapid urbanisation. Blue spaces have long been considered a possible mitigation strategy to ameliorate the UHI. However, our knowledge regarding the interaction of waterbodies with their urban surroundings is still limited. This review attempts through a comparative analysis of the available literature to examine the thermal effects of static blue spaces on the urban climate. Remote sensing studies are the most common approach analysed in this review but there is a clear disparity between the cooling potentials reported by remote sensing as opposed to field measurements or numerical simulations, likely due to a lack of nocturnal measurements, when warming due to thermal inertia can occur and consideration of the latent heat flux. The size and shape of blue spaces are shown to be important variables for the cooling achieved in urban settings but there is no consensus in the literature. This is likely due to the different locations and climates of the studies, it can be hypothesised that in locations with an even distribution of wind directions a rounder waterbody is more effective while in locations where wind direction is more uniform an elongated waterbody aligned to the wind is more effective due to the increased fetch. From the analysis of the literature, it is clear that there is still a distinct knowledge gap regarding the physical interpretation of waterbodies' contribution to the urban climate. There is also a current lack of information about the diurnal and seasonal variability of the various structures and processes. There is evidence, however, that the comfort achieved by sensible cooling can be offset by the increased water vapour content and that during the night blue spaces may actually exacerbate the UHI, reducing urban thermal comfort.

Highlights:

- The influence of urban blue space on urban canopy/boundary-layer temperatures
- The cooling effect of blue spaces varies with time of day, the season and location
- Remote sensing studies tend to overestimate the cooling potential of blue space
- Blue spaces may not provide cooling all day long and may provide warming at night
- The influence of geometry and diversity of urban blue spaces requires more research

1. Introduction

Today, more than half the world's population lives in cities and this percentage is expected to increase to 68% by 2050 (United Nations, 2018). There is, therefore, the need to study the impact of the urban environment on human health and well-being. This upward trend of urbanization, both in terms of area

and density, affects the radiant balance of urban areas, anthropogenic heat release, wind flow and the convective heat exchange between the built environment, its rural surroundings and the atmosphere above. This can lead to a substantial intensification of the UHI (Memon et al., 2008; Oke, 1987), i.e. the characteristic warmth of the city compared to its rural surroundings.

The UHI can be likened to a bubble of air situated over a city arising from changes in surface roughness, convection efficiency and the latent to sensible heat balance. This bubble of air, isolated from the rest of the atmosphere is typified by decreased vertical transport of air, trapping warm air and pollutants at street level. Despite being apparent in all seasons, the effect is greatest during periods of calm, still weather (anticyclonic – high-pressure) such as heat waves, when higher air temperatures and increased shortwave solar flux, increase daytime heat storage to be reradiated at night (Grimmond et al., 2010; Oke, 1987). Projections of climate change indicate that the frequency and severity of such extreme weather events will increase in the future (IPCC, 2014), leading to increased heat-related and respiratory illnesses, increased cooling energy demand for buildings and deterioration of thermal comfort conditions in urban centres. As an example, the UHI for London is ~8 °C and has serious implications for building energy use and human health (Kolokotroni et al., 2006; Tomlinson et al., 2011).

It is possible that this effect could be manipulated through the introduction of green and blue infrastructure networks to cities (parks, trees, ponds, watercourses, etc.), altering the aerodynamic properties of the cityscape and increasing evapotranspiration, promoting the vertical transport of heat, air and pollutants (Arnfield, 2003; Gunawardena et al., 2017). In addition, according to a recent study (Chan et al., 2017), the existence of water ponds and trees in parks can enhance the thermal acceptability, i.e. the state of mind that is in acceptance with the surrounding thermal conditions, which can be attributed to the positive psychological response of humans to green and blue features, especially during summer (Berglund, 1979). Although green spaces have been studied to a reasonable extent by several researchers, there seem to have been only a few studies that address the potential of blue infrastructure to ameliorate the UHI (Koc et al., 2018). Henceforward, the terms ‘blue spaces’, ‘blue infrastructure’ and ‘waterbodies’ will be used interchangeably and will refer to outdoor urban surfaces that are predominantly dominated by water, e.g. lakes, rivers, ponds, fountains etc. It has been found that blue spaces can generate a cooling effect of 1-3 °C within their vicinity (~30 m) (Kleerekoper et al., 2012), indicating a potential to mitigate the thermal environment. However, such measurements are often limited and there is little information regarding the wider impacts of blue infrastructure on the citywide UHI, either horizontally or vertically.

Arnfield’s (2003) work was one of the first to address the lack of studies that assess the water budget in cities, preparing the field for further research in this area. Earlier, Martínez-Arroyo and Jáuregui (2000) had suggested the implementation and adequate distribution of small inland blue spaces in Mexico City to ameliorate the urban environment but provided little detail regarding expected magnitudes. Coutts et al. (2012) analysed the potential of waterbodies to provide cooling and comfortable conditions in Australian cities but only in terms of Water Sensitive Urban Design (WSUD), the equivalent to Sustainable Urban Drainage Systems (SuDS) in the UK. In 2014, the Chinese government launched the ‘sponge city’ project in order to tackle urban flooding and waterlogging of several cities across the country. This included the implementation of permeable pavements, water ponds, green roofs and wetlands among others. Although the understanding of the contribution of water bodies was still vague, these measures led to a decreased UHI intensity in the city of Changde by 0.92 ˚C (He et al., 2019a). Völker et al. (2013) conducted a meta-analysis of 19 papers (27 case-studies), compiling empirical findings from both static and dynamic waterbodies, assessing the temperature effects of blue spaces compared to a reference urban area without any blue space. This showed that the median temperature difference was 2.5 °C, indicating a strong cooling effect. Nonetheless, the studies included in the review obtained temperature data either from in-situ measurements or remote sensing measurements, with the latter only able to capture surface radiant temperatures, mainly of large bodies of water, i.e. lakes or rivers, and only at a specific moment in time. A more recent analysis of the literature has shown that urban blue spaces do not necessarily act as a cooling agent over the whole day since their surface can reach higher temperatures than their urban surroundings at night or early morning, producing a warming effect (Manteghi et al., 2015). Focusing mainly on studies that involve

technologies based on the evaporation of water, e.g. sprinklers, water curtains, or fountains, which are implemented in public spaces to mitigate heat stress, Santamouris et al. (2017) concluded that on average, water-based techniques provide an average cooling effect of 1.9 °C and the higher the air temperature the higher the cooling potential. Gunawardena et al. (2017) studied the thermal effects of blue infrastructure in relation to the urban canopy and boundary-layer temperatures. Their meta-analysis revealed a lack of studies based upon air temperature monitoring and that, under thermally oppressive conditions, blue spaces may provide nocturnal warming, further impacting thermal comfort and human health. Along the same line of thought, this study analyses the existing literature with regards to the thermal effects of different blue spaces in the urban environment. This analysis is performed with respect to the methodology used, the background climate and the variables studied, in an effort to reveal trends between the existing studies and pinpoint future research opportunities.

In order to compare disparate studies of the influence of blue spaces on the urban climate, we need to have an understanding of the formation of the different atmospheric structures above an urban area. The turbulent exchange between the urban surfaces (e.g. buildings, roads, blue and green spaces) and the atmosphere defines the distinct climatic conditions close to the ground (Oke et al., 2017). Hence, the comprehension of the airflow within the different atmospheric layers is central, given that turbulent motion is the primary mechanism that transfers momentum, heat, water vapour and air pollutants to and from a surface. The following section summarises the atmospheric processes that give rise to the boundary layers above an urban area and ultimately the urban heat island and how these vary over the course of a day.

2. Boundary-layer atmospheric structure above cities

2.1 The planetary boundary layer

The lowest part of the atmosphere that is in contact with the Earth's surface is termed the Planetary Boundary Layer (PBL) (Stull, 1988). In general, a layer of fluid can be considered as a boundary layer if its transfer properties are determined by the properties of an underlying surface. Depending on the season and the time of the day, the PBL's depth can vary between ~100 and ~3,000 m, extending from the surface up to the *free atmosphere* where atmospheric properties are independent of the Earth's surface. The parameters affecting this diurnal and seasonal cycle are thermal atmospheric mixing, the surface roughness, the presence of air pollutants and moisture content (Oke et al, 2017). The lowest part of the PBL (approximately 10%) is termed the *surface layer*, where friction with the Earth's surface dictates the flow characteristics.

After sunrise, solar radiation heats the surface and thus gives rise to buoyancy-driven thermals that causes air to rise to the top of the PBL where a *capping inversion* prevents further lifting. During the daytime, the upper part of the PBL termed the *mixed layer*, accounts for approximately 90% of the PBL. Inside the mixed layer, atmospheric properties, such as potential temperature, wind speed and water vapour, are well mixed by turbulence and present little variation with height as shown in Figure 1 (Driedonks and Tennekes, 1984; Srivastava et al., 2010). The upmost part of the mixed layer is an *entrainment zone*, where overshooting thermals and intermitted turbulence are present (Driedonks and Tennekes, 1984; Stull, 1988). The top of the mixed layer is usually defined as the level where the capping inversion is strongest, i.e. the middle of the entrainment zone, or the level of the most negative heat flux (Tombrou et al., 2007). During the night, when the PBL has constricted to some hundreds of metres near the surface, the heat loss from the ground creates a stagnant layer, which reduces vertical mixing. Above this nocturnal boundary layer, a mixed layer with properties similar to that of the previous afternoon is formed. This is known as the *residual layer*, which extends up to the height of the daytime PBL and is capped by the inversion preserved from the daytime entrainment zone. Despite being well mixed, there is a little active mixing inside the residual layer.

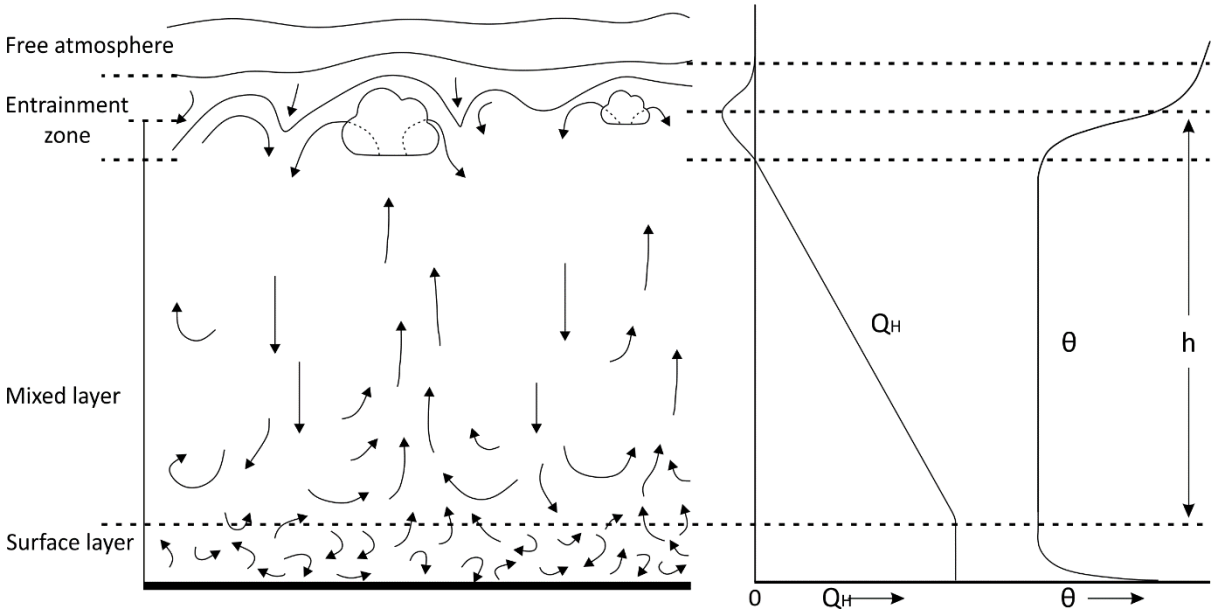

Figure 1: Illustration of the airflows inside a mixed layer during daytime and the associated vertical profiles of the sensible heat flux density (Q_H) and potential temperature (θ). The depth of the mixed layer is denoted by (h). Based on Oke (1987).

2.2 The urban boundary layer

As air flows towards a city, the increased roughness of the urban structure (buildings, trees and block-scale features) cause the structural distortion of the rural PBL leading to its partitioning. An internal boundary layer is formed, namely the Urban Boundary Layer (UBL), whose internal structure by day and night can be seen in Figure 2. The UBL is governed by mesoscale (hundreds of metres) processes and extends from the ground to a height where atmospheric properties (wind velocities, temperature gradients and vertical fluxes) are independent on the presence of the urban area at its lowest boundary. The urban surface is typically slower to warm than its rural counterpart, but ultimately reaches higher temperatures over the course of the day. This leads to enhanced mixing inside the mixed layer and thus increases the height of the capping inversion compared to the one found in the rural PBL (Figure 2b). At night, the height of the nocturnal UBL is considerably lower than during the day and primarily depends on the cities' surface roughness and strong nocturnal UHI (Figure 2a). Stability conditions (stable, unstable and neutral) affect the structure and depth of the UBL and consequently the temperature, velocity and turbulence intensity profiles within it (Marucci et al., 2018).

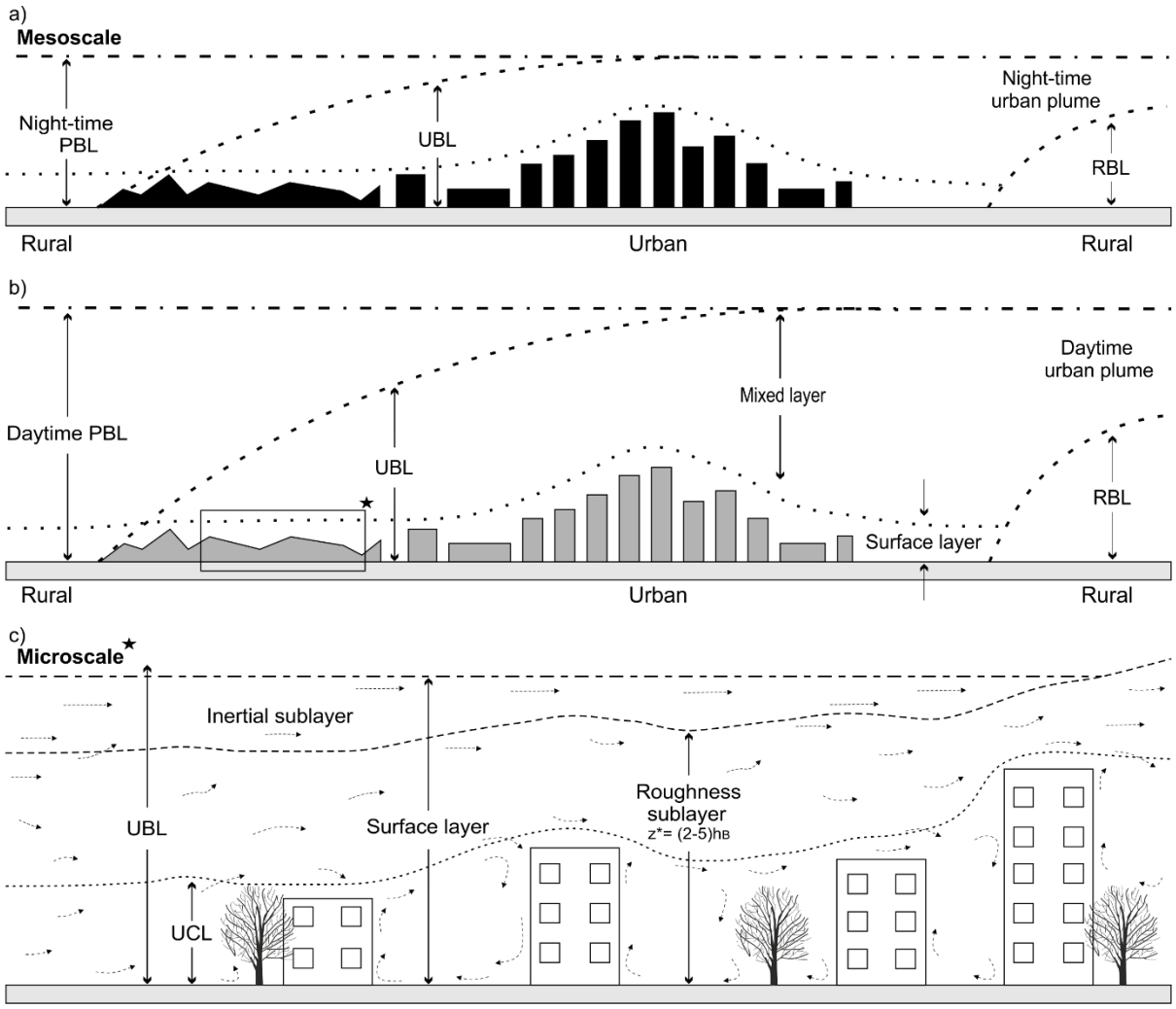

Figure 2: Boundary-layer structure over a city resulting from the transition to increased surface roughness: a) Night-time boundary layers, b) Daytime boundary layers, c) Microscale vertical structure of the surface layer (h_B is the average building height). Based on Oke (1987).

Airflow over the urban domain leads to increased wind drag and turbulence, reducing wind velocities and deepening the zone of frictional influence. This process is responsible for increased vertical motion, which consequently forms a relatively shallow *roughness sublayer* above cities, extending up to a level of about two to five times the average height of buildings (Barlow, 2014; Oke, 1987; Raupach et al., 1991). Mechanical turbulence is, thus, the dominant driver along with the reduced wind velocities, and both properties are strongly affected by the height and spacing of the urban roughness elements and the urban configuration. Inside the roughness sublayer, the wind shear stress is not constant, starting from zero in the upper part of the canopy, reaches its highest value at some distance above the tops of the buildings (Kastner-Klein and Rotach, 2004).

The combined effects of an urban district lead to the formation of a horizontally homogeneous layer right above the roughness sublayer: the *inertial sublayer*. These two layers constitute the surface layer over an urbanised area. Contrary to the roughness sublayer, mean atmospheric properties are relatively homogeneous horizontally, while the vertical wind speed is negligible, something that has led the inertial sublayer to be known as a *constant flux layer* (Barlow, 2014; Raupach et al., 1991). Note that the presence of the inertial sublayer is dependent on the physical structure and regularity of the city.

2.3 The urban canopy layer

The lowest part of the roughness sublayer is the Urban Canopy Layer (UCL) that extends from the Earth's surface to around the height of the tops of trees and buildings. The UCL is a microscale (tens

of metres) concept where the local climatic conditions are influenced by the different surface properties and geometries of the urban environment. Within this layer, different processes can be observed near the upper part, i.e. the tops of buildings, and inside the canopy itself. In particular, within the street canyons, the decreased sky view factor and the increased height to width ratio may lead to the obstruction of incoming shortwave solar radiation, trapping of the outgoing longwave radiation (heat) and the sheltering from the prevailing winds. In contrast, at the roof-level mixing and wind shear stress are the dominant processes. As depicted in Figure 3a, when the canyon aspect ratio is small ($H/W < 0.35$), buildings form individual wakes, which largely dissipate before impinging on the next building in the array. In these isolated roughness flows the concept of the urban canopy is of limited use. As the building spacing reduces ($0.35 < H/W < 0.65$), the vortices at the leeward side interfere with the flow down the windward side of the next element (Figure 3b). In highly dense areas ($H/W > 0.65$), the vertical mixing may be restricted due to the aerodynamic isolation of urban street canyons from the overlying airflow with the urban canopy concept becoming fully developed (Figure 3c). Under this skimming flow regime, recirculation vortices are created that reduce the mean canyon velocity and thus restrict the momentum exchanges between the UCL and the atmosphere above roof level, trapping pollutants inside the urban canyon (Kastner-Klein et al., 2004; Oke, 1988).

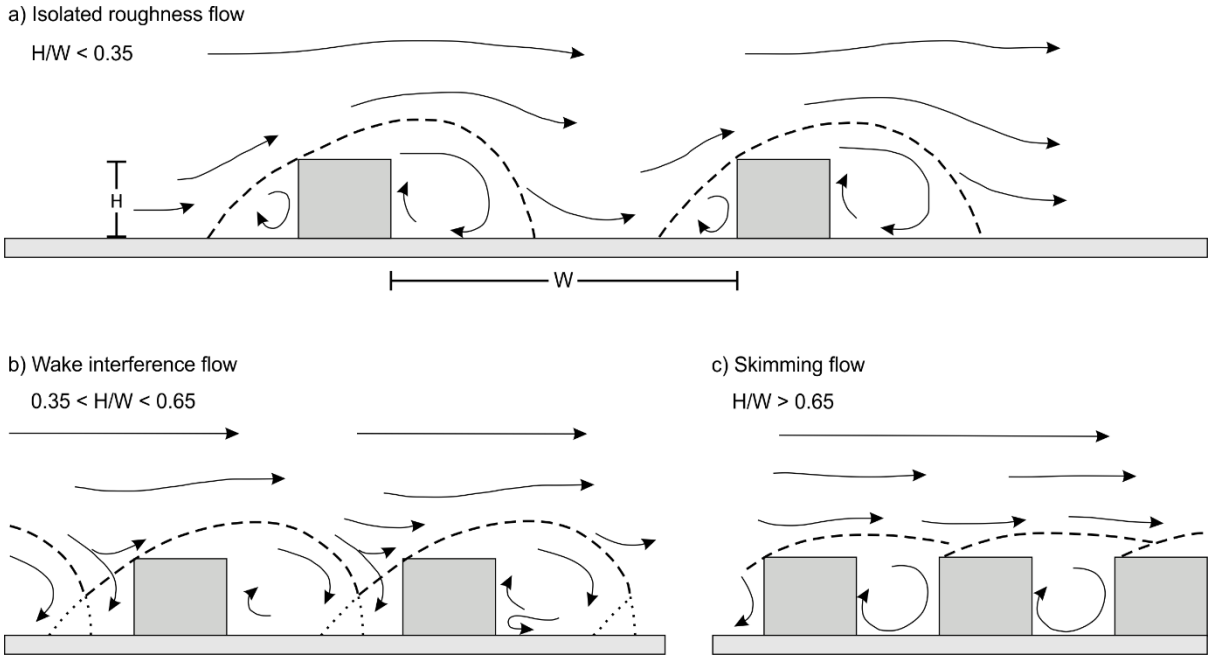

Figure 3: Different flow regimes over building arrays of the same height based on the canyon aspect ratio (H/W). Modified after Oke (1988).

Figure 4 illustrates how the wind profile changes vertically and horizontally with height as air flows from a relatively smooth surface (e.g. a rural area) to a rougher urban area. A summary of the boundary-layer atmospheric structure and its scaling variables above cities is given in Table 1.

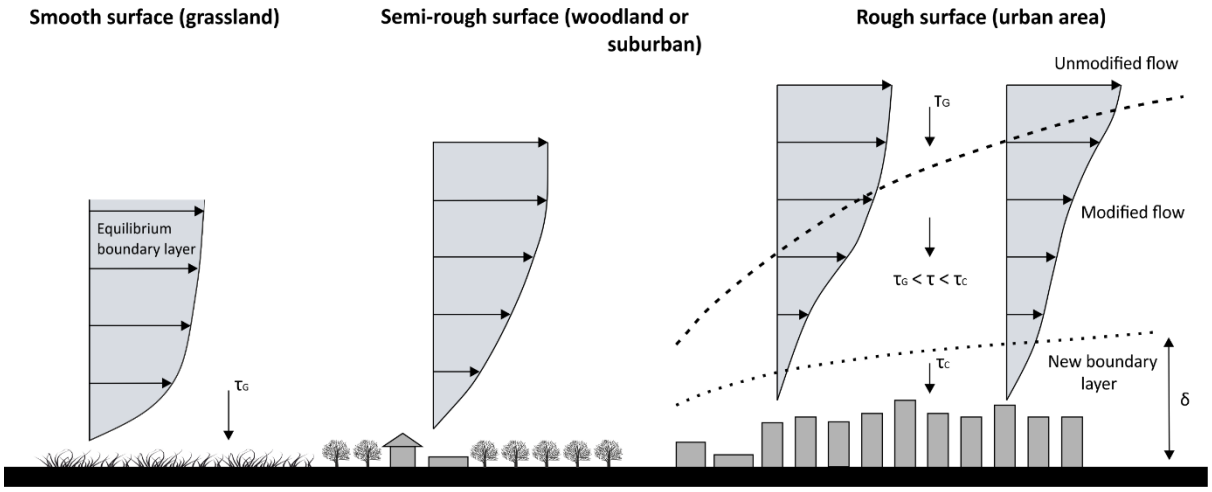

Figure 4: Variation of the velocity profile as air flows from a smooth surface to a rougher surface and the development of a new boundary layer (dotted line in the urban area). The dashed line represents the boundary between the modified and unmodified flow. The vertical momentum flux in the modified flow is between τ_G (flux in the unmodified flow) and τ_C (flux below the height δ). Based on Monteith and Unsworth (2013) and Oke (1987).

Table 1: The vertical structure of the urban climate system based on typical length scales. Based on Oke (1984).

Layer	Definition	Dimensions	Scale
Urban Canopy Layer (UCL)	• From the ground to the mean height of buildings and trees	Tens of metres	Microscale
Roughness sublayer	• From the ground up to two to five times the height of buildings and trees • Includes the UCL • Flow is affected by individual elements	Tens of metres	Microscale
Inertial sublayer	• Above the roughness sublayer • Small variation of turbulent fluxes with height (<5%)	~25 – 250 metres	Local
Surface layer	• Includes the UCL, the roughness sublayer and the inertial sublayer • Flow is dominated by friction with the Earth surface	~300 metres	Local
Mixed layer	• Above the inertial sublayer • Atmospheric properties are well-mixed by thermal turbulence • Usually halted by a capping inversion	~250 – 2,500 metres	Mesoscale
Urban Boundary Layer (UBL)	• The entire layer between the ground and the top of the mixed layer	Hundreds of metres	Mesoscale

2.4 Urban heat island types

The formation of the UHI can be described in terms of the nature of the climate in either the UBL (UHI_{UBL}) or the UCL (UHI_{UCL}). Although closely coupled, heat islands within the UBL and UCL are generated by different processes and have different magnitudes (Oke, 1995). Therefore, an understanding of the formation and properties of each layer is highly recommended in order to assess the mitigating potential of urban blue space. However, since this is beyond the scope of this paper the reader is referred to Table 2 and more detailed textbooks on that subject .

The UHI_{UCL} is the difference between the air temperature near the ground (below roof level) in the city with the corresponding one in the rural counterpart at the same height. Its magnitude depends on the time of the day and year as well as the background weather. It reaches its peak at calm, cloudless nights because of the relative difference in the nocturnal cooling rates of air above urban and rural

surfaces. Additionally, the greater the canyon aspect ratio (H/W) the greater the UHI_{UCL}. During daytime, the UHI_{UCL} is usually negligible or even negative (Oke et al., 2017).

The UHI_{UBL} is the difference between the air temperature within the layer that extends from the top of the UCL to the top of the UBL, with that of the PBL in the countryside in similar height. Its depth depends on the stability of the surrounding area, the magnitude of the urban heat flux and wind speed (reversely) among others. The UHI_{UBL} is much less observed than the UHI_{UCL} since it requires very tall towers, balloon or aircraft measurements (Oke et al., 2017). The greatest temperature differences are found at night, when the urban landscape continues to emit accumulated heat due to the high thermal inertia of the materials and the urban canyon effect. At the same time, rural temperatures have reached their nadir as they can easily lose accumulated heat by means of evaporation, convection and radiation. Once the surfaces have cooled, warmer air in the atmosphere above creates a downward flux resulting in the contraction of the urban boundary layer to often <100 m.

Table 2: Possible causes of the different UHI in the UBL and UCL. Based on Oke (1987).

Energy processes leading to a positive thermal anomaly	
Urban boundary layer	Urban canopy layer
Increased absorption of solar radiation	Increased absorption of solar radiation
Anthropogenic heat release	Increased heat storage
Increased sensible heat flux from above[1]	Anthropogenic heat release
Increased sensible heat flux from below[2]	Reduced evapotranspiration
	Increased absorption and re-emission of longwave radiation
	Reduced longwave radiation loss
	Reduced turbulent mixing

[1] This can be attributed to warmer air trapped inside the capping inversion layer.
[2] Meaning the UCL.

2.5 Blue space – atmosphere dynamics

Having considered how the structure and properties of an urban area give rise to the partitioning of the atmosphere and the various properties of the different layers, we can begin to examine how blue spaces which can be both a source of cooling (due to evaporation), a source of heating (due to thermal inertia) and produce water vapour (which is less dense than air), may affect the partitioning of the atmosphere above an urban area.

Urban areas, which are relatively drier than the rural ones, would allegedly present lower values of moisture content than their rural counterpart. However, it has been shown (Kuttler et al., 2007; Lee, 1991; Mayer et al., 2003) that cities can be moister than their rural surroundings especially during summer nights and in winter. This phenomenon is known as urban moisture excess and can be positively related to the intensity of the UHI, often with a phase difference of few hours (Holmer and Eliasson, 1999; Kuttler et al., 2007; Mayer at al., 2003), albeit this interrelationship is an ongoing debate (He et al., 2020a, b; Yang et al., 2020) and more evidence is needed. In general, evaporation from a blue space requires supply of energy, water-to-air vapour gradient (vapour pressure deficit) and sufficient turbulence to maintain this gradient. Therefore, at calm and clear nights, when turbulence is relatively weak, the presence of an urban blue space would be expected to further increase the water vapour content of the canopy layer air, leading to an intensification of the UHI. This warming effect will be discussed in more detail in the following sections. It has become apparent that in order to gain full understanding of the blue space effects on the UCL, apart from the temperature, wind and turbulence vertical profiles, knowledge of humidity profiles is also important. Nonetheless, this is a subject that has received less attention compared to the study of other UCL quantities (Yang et al., 2020).

When a blue space is embedded in the drier urban core, an oasis effect can be observed by daytime. Being relatively cooler, its presence can induce subsidence of drier air from the mixed layer down to

the surface layer, meaning that that heat is extracted from the warmer air above towards the cooler water surface. This creates a retained positive feedback mechanism, where the latent heat flux (Q_E) exceeds the available radiant flux (Q^*) (Oke et al., 2017). However, evaporation is not only dependent on the surface characteristics. During the daytime, thermals originating at the ground can enhance coupling between the surface layer and the warmer, drier top of the mixed layer. This can lead to warmer, drier air to be transported near the ground, increasing the vapour pressure deficit and thus boosting evaporation. During the night, water may become warmer that its surrounding urban landscape causing warm, moist air to be advected towards the city. This diurnal circulation of wind in the locality of a waterbody can be described as a waterbody-breeze system, similar to a daytime park-breeze system and a night-time land-breeze system (Gunawardena et al., 2017). The implications of this hypothesized centripetal system will be discussed later.

Growth and depth of the UBL is determined primarily by the sensible heat flux (Q_H) (Barlow, 2014), which in turn is dependent on the partitioning of turbulent fluxes into Q_H and Q_E. This proves to be particularly important if one desires to accurately represent the influence of blue spaces. A recent study suggests that during hot summer nights only a small part of the released heat from a waterbody is related to sensible heat (11%) (Solcerova et al., 2019). This finding underlines the need to extend research on the diurnal (especially night-time) energy balance of blue space in order to shed some light on its thermal behaviour and the potential to ameliorate the UHI.

3. Blue space effects on the urban environment

Waterbodies can be categorised into two different groups according to their fluid flow characteristics: static (closed) and dynamic (open). Static waterbodies can be in turn categorised into ponds and lakes. Normally, urban ponds are shallower and smaller in size than lakes. The median pond surface area is 4,000 m², while lakes range usually between 50,000 and 300,000 m² (Kalff, 2002). Small static waterbodies are usually considered those with an area <100,000 m² (Downing, 2010). Regarding shape, ponds usually present a smaller surface-area-to-perimeter ratio and thus are more of an irregular shape (Song et al., 2013). While, dynamic blue spaces that can be found in cities are mainly rivers, canals and streams.

3.1 Surface controls

The cooling effectiveness of blue spaces is positively correlated with the water-to-air temperature gradient and the net-radiation balance, while it is also related to the potential of evaporative conversion and atmospheric advection (Hathway and Sharples, 2012). For dynamic waterbodies, the impact of fluid flow characteristics may also play an important role in the spatial distribution of heat release, since stored energy can be transferred downstream by advection (Hathway and Sharples, 2012). However, for relatively shallow and small urban streams, heat inputs from instream discharges, surface runoff and groundwater exchange may be of importance in regulating the energy partitioning (Gu et al., 1998; Webb et al., 2008). Given the limited movement of water, static waterbodies tend to be more sensitive to water-to-air thermal exchanges.

The radiation budget of waterbodies is associated with the albedo at a given time. Although the albedo of a water surface is considered low (~0.08 for large latitudes) (Paulson and Pegau, 2001), its value changes depending on the solar angle, the wavelength of solar radiation, the roughness (waviness) of the water surface and its biochemical composition. Solar radiation that penetrates into the water may be absorbed as heat, scattered or transformed into other energy sources (Lampert and Sommer, 2007). Shortwave solar radiation can usually penetrate to a depth of ~10 m, while longwave radiation (e.g. infrared ~10 μm typical of radiated heat in the anthroposphere) is almost entirely absorbed and transformed into heat (Oke, 1987).

The high thermal inertia of water leads to a small diurnal change of the water surface temperature leading to a nearly constant outgoing flux of longwave radiation through the day. In addition, although water has a relatively high thermal conductivity compared to other liquids (0.598 W/m-K at 20 °C), heat transport by means of molecular diffusion in a motionless lake is negligible (Lampert and Sommer,

2007). One may notice that this means that the absorbed radiative flux leads always to a warming of the upper layers of a waterbody, and hence water temperatures decrease exponentially with depth, something that contradicts with the small water surface temperature variations (see Figure 5). The physical explanation of this 'paradox' is hidden in the processes of the deep penetration of solar radiation, mixing of water by convection and mass transport, and evaporation; the former two help heat to be spread throughout a larger volume, while the latter intensifies instability and thus thermal mixing (Oke, 1987). Another factor that affects the water surface temperature is the turbidity of the water (and the resulted temperature stratification), which is often not taken into account in numerical studies. In fact, this might play a significant role to the observed discrepancies between measurements and simulations (Solcerova et al., 2019).

The surface inhomogeneity of cities creates microscale and local advection. This can also be the case for patches of urban blue space, whose different surface properties create sharp gradients at the transition borders, enhancing or hindering surface flux depending on the magnitude and sign of these gradients (Oke et al., 2017). When air passes from drier, rougher urban surfaces over wetter, smoother waterbodies, there is a sharp increase in latent heat flux, and thus evaporation, as advection of dry air increases the water-to-air vapour gradient (Bünzli and Schmid, 1998). This is known as the moisture leading edge effect, which may lead to the formation of a local internal boundary layer where flow is in equilibrium with the underlying surface (Barlow, 2014).

3.2 Atmospheric controls

A waterbodies' ability to affect the surrounding urban environment is principally dependent on the local environmental and weather conditions, such as ambient temperature, humidity, wind speed and direction, as well as the inherent properties of the water, i.e. specific heat capacity, enthalpy of vaporisation etc. One of the most recorded thermal effects of blue spaces is the evaporative cooling potential, meaning the transformation of sensible heat into latent heat of vaporisation. The addition of water vapour in the atmosphere can enhance vertical transport since water vapour is less dense than air. During the first few hours after sunrise, absorbed shortwave radiation warms the water increasing its stored energy. This leads to a maximum water surface temperature towards the afternoon, when the water-to-air vapour pressure deficit also peaks, inducing a strong evaporative flux. The increased heat storage capacity of water can maintain the evaporative flux well into the night. Relatively strong winds above the water surface will increase evaporation and may increase the cooling effect, while increased water vapour content limits evaporative heat loss and may lead to a decreased cooling effect (Stathopoulos, 2006; Webb and Zhang, 1997). The latter is linked with the amount of moisture that can be added to the atmosphere, i.e. the water-to-vapour pressure deficit. At this point it is useful to mention that relative humidity, which is often used by researchers in urban studies, is a measure of how close the air is to saturation at a given temperature and not a measure of vapour deficit or moisture content. For relatively shallow waterbodies the evaporative flux experiences a diurnal cycle, while for larger bodies (e.g. oceans) it is characterised by seasonal variations (Oke, 1987). The high thermal inertia of water allows urban blue spaces to mitigate the thermal environment by acting as thermal buffers, although the whole waterbody's thermal inertia is not always accessible, as will be demonstrated later (Oke, 1987). In addition, the analysis of the existing literature in the following chapters will highlight that only a few studies address this issue.

3.3 Effects of water stratification

A static waterbody that absorbs solar radiation and receives heat inputs from the overlying atmospheric layers can result in what is known as thermal stratification (Kalff, 2002; Van Buren et al., 2000). The term implies that the water column is divided into layers of different temperature and density (Figure 5). Water reaches its maximum density at 4 °C and thus can become less dense by either warming or cooling. However, the density difference is largest in higher temperatures, e.g. the density difference of water between 24-25 °C is 30× greater than the density difference between 4-5 °C (Lampert and Sommer, 2007). When warmer water is concentrated near the surface, the density change per degree centigrade can lead to increased resistance to mixing, i.e. stability of the water column. Wind

shear stress can only produce effective mixing over a limited depth, leading to the formation of a sharp boundary between a shallower mixed layer and the deeper colder waters. In such stratified bodies, the warm water surface layer, termed epilimnion, is responsible for heat exchange with the atmosphere. This indicates that the thermal capacity of the entire water volume is not always accessible for energy exchange. Between the epilimnion and the unmixed colder water (hypolimnion), a sharp temperature gradient is formed, the thermocline. The region of the greatest temperature change, which separates the two layers, is called metalimnion.

Based on the latitude and depth, waterbodies present different annual temperature profiles. Lakes in temperate latitudes experience stratification during summer and winter, while in spring and autumn overturning occurs, meaning that a homothermic profile is developed, with the same temperature throughout the water volume (Lewis Jr, 1983). Depending on the season, buoyancy-driven overturning may occur when the water surface temperature is above or below the 4 °C threshold. In spring, as the water in the epilimnion starts to warm and approaches 4 °C, it increases in density and colder water rises to the top. At this point, a strong wind can potentially lead to a fully mixed waterbody, initiating the spring overturning. Any further warming increases the differences in density and the lake begins to stratify, restricting vertical mixing (Oke, 1987). However, before summer stratification is fully established, strong mechanical energy provided by wind shear stress can enhance the mixing of the water column and erode stratification (Boehrer and Schultze, 2008), but after a short time, the epilimnion becomes stably developed. On top of that, the fast warming of the shallower water at the littoral zone of a waterbody may lead to the creation of a diurnal current that drives warmer water to the open water area, albeit it cannot destabilise the overall stratification (Stefan et al., 1989). It is noticeable that the thermally active zone of a stratified waterbody reaches its maximum thermal capacity in late summer when the warming has extended to greater depths (Gunawardena et al., 2017). In autumn, as the water begins to cool and increase in density a reverse overturning takes place. This seasonal change of stratification and overturning in lakes in temperate can happen during one day in tropical lakes, implying the importance of location when trying to assess the impact of blue spaces.

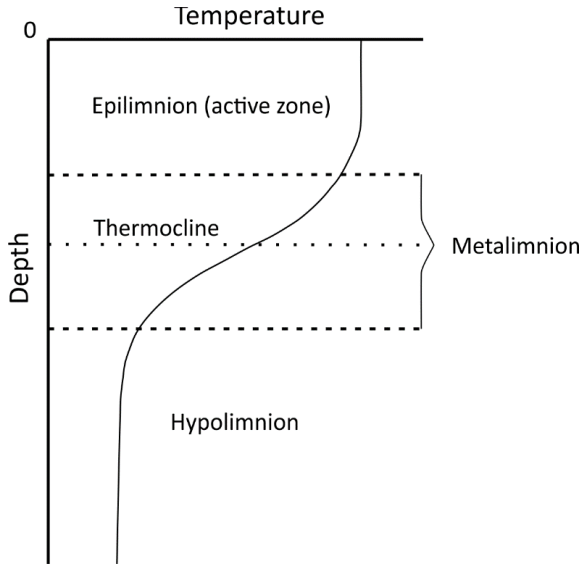

Figure 5: Illustration of a typical temperature profile during summer in a lake at temperate climates. Based on Lampert and Sommer (2007).

Shallow static waterbodies, which are usually encountered in cities, have been typically described as well mixed, with their epilimnion extending throughout the entire water column. This absence of stratification has been attributed to the higher potential for wind-driven mixing. However, recent studies have shown that even shallow bodies (<3 m) (Brans et al., 2018) can exhibit prolonged and repeated stratification, i.e. temperature gradient > 1 °C measured from the top to mid-depth, under warm and calm weather conditions (Abis and Mara, 2006; Song et al., 2013). In particular, Song et al. (2013) showed that, during the middle of the summer, shallow urban ponds in Canada (Dfb) present up to 4 °C temperature differences between the top and the bottom layers, indicating a well-established

stratification. They related this phenomenon to the low wind velocity and the increased level of suspended materials, which increases the absorption of shortwave solar radiation. Using a Computational Fluid Dynamics (CFD) model of a small shallow lake (average and a maximum depth of 1.1 m and 4 m, respectively) in Ghana, Abbasi et al. (2016) found that during the night (24:00) the entire water column was well-mixed. However, at 14:00, when the air temperature reaches its peak, the vertical temperature profile of the waterbody indicated temperature differences between the top and a depth of 1.5 m of approximately 2 °C. The main contributors to stratification were the turbidity of the water (calculated from measured Secchi depths) and the inclusion of turbulence in the CFD model (Abbasi et al., 2017b). Song et al. (2013) also found that depth and shape factor (surface area to perimeter ratio) are the two geometric parameters that affect stratification the most, with the maximum depth to demonstrate the strongest correlation. Therefore, the depth of the epilimnion, i.e. the thermally active zone of a waterbody, can theoretically reduce the water-to-air temperature gradient and thus limit the overall cooling potential. However, evidence is yet weak to draw safe conclusions and further research is needed.

3.4 Impact quantification

There are two distinct methods to study the urban climate, and consequently to assess the impact of a waterbody on the thermal environment: observation and simulation approaches (Mirzaei and Haghighat, 2010). Observational studies include field measurements, experimental studies, e.g. reduced-scale physical models or wind tunnels, and remote sensing. Until recently, studies that involved the contribution of static waterbodies to their urban microclimate have mainly used field measurements and remote sensing. However, more recently, numerical modelling has been proven to be another powerful tool to examine the urban climate due to its ability to isolate different influencing parameters and assess their relative importance to the urban context. This review will study these approaches in relation to the type of urban blue space and the inclusion of different waterbody's characteristics, such as depth, shape, spatial distribution etc. This paper only considers the thermal effects of static waterbodies as dynamic waterbodies are too dependent upon locality and upstream influences and there is too little literature to draw sufficient conclusions.

4. Field measurements & experimental studies

On-site or field measurements include special monitoring equipment and sometimes can be labour-intensive. There are two main types of on-site monitoring techniques. The first includes measurements at fixed stations, such as conventional weather stations that provide long-term climatological information, while the second is short-term field campaigns, including fixed observing sites and flow-following or mobile measurements. Despite the relatively straightforward technique, these can reveal the reduction of air temperatures or the increase of humidity near and/or above an urban blue space with good accuracy. Assessing the real complexities of the problems involved is actually their greatest advantage (Blocken, 2015). Luke Howard, using instruments installed on his property, was the first to record that London was approximately 0.2 °C and 2 °C warmer than its rural surroundings during the day and night, respectively (Howard, 1833). However, since these studies rely on meteorological and geometrical conditions of the examined area, they can only provide information about the local thermal environment of the examined area and at a limited number of points in space. In addition, although it is possible to collect data from different points in time, it is rather hard to come to a reliable conclusion regarding a prolonged period. The accuracy of the measurements is also subject to the quality of the instrumentation and the accuracy of the sensors used.

One of the first studies that measured the cooling effect of an urban pond was conducted in Fukuoka, Japan (Cfa) by Ishii et al. (1991) who found an air temperature reduction of 3 °C. Later, Nishimura et al. (1998) carried out a similar study in Osaka, Japan (Cfa) for two consecutive typical summer days under clear sky conditions during the daytime. Results showed a decrease of up to 2 °C on the leeward side of the pond. Similarly, Chen et al. (2009) found that measurement points near an artificial lake in Guangzhou, China (Cfa) can be up to 2.2 °C cooler than their urban surroundings. A higher cooling effect, approximately 3 °C, was observed by Li and Yu (2014) who carried out a field campaign in

Chongqing, China (Cfa) for three urban lakes with different sizes (8,800 – 69,600 m²) and different land shape index (LSI). The LSI is a dimensionless number defined as:

$$LSI = \frac{P_t}{2\sqrt{\pi \times A}}$$

Where P_t is the total perimeter and A is the area of the waterbody. Therefore, a circular lake would have an LSI of 1. Their analysis addressed the influence of the shape and area of the blue space, concluding that the smaller the LSI (or the rounder the shape) the greater the cooling potential.

Xu et al. (2010) attempted to assess the impact of a lake (87,000 m²) on the thermal comfort at pedestrian level in Shanghai, China (Cfa). They found a significant decrease in heat stress in the first 10-20 m from the lake's edge. However, since the lake is located inside a larger park, the study only really highlights the potential of synergistic cooling, where green and blue space jointly affect the urban environment. Recently, for a similar climate in Brazil (Cfa), Targino et al. (2018) found that Igapó Lake was found to be warmer than the neighbouring green park throughout the course of the day, but relatively cooler than the urban environment. It should be mentioned that measurements were conducted during late autumn. The higher cooling potential of green parks was also mentioned in Li and Yu (2014); the authors however considered the comparison in isolation without accounting for the integrated dynamics between the two features. Field observations for a small pond (40,000 m²) in Tel Aviv, Israel (Csa) showed an ambient temperature reduction of almost 1 °C during midday hours, indicating that even small blue spaces can provide cooling effects. The study was conducted under hot-and-dry and hot-and-humid summer conditions (from 07:30 to 19:00), revealing an unpleasant warming effect after 15:30 due to increased moisture content and small or reversed temperature differences, meaning that the water surface temperature had risen higher than that of the overlying air (Saaroni and Ziv, 2003). Huang et al. (2008a, 2008b) and Yang and Zhao (2016) also found that water areas can be up to almost 1 °C warmer than the surrounding concrete surfaces in the early morning (06:00) and midnight, although they generally provide cooling during the day. Steeneveld et al. (2014) were led to similar results in a study of the UHI for several cities in the Netherlands (Cfb), combining data from 18 hobby meteorologists and a fixed station network in Rotterdam. In particular, it was shown that the 95th percentile of the daily maximum UHI increases with the available open water surface. Heusinkveld et al. (2014) came to qualitatively similar conclusions in their mobile measurement study in Rotterdam (Cfb), indicating that waterbodies can have a negative impact on the thermal environment during the night and increase the maximum UHI. The authors studied both static and dynamic waterbodies, but the relative contribution could not be obtained.

Considering the need to focus more on the night-time thermal behaviour of urban waterbodies, Solcerova et al. (2019) analysed data from a field campaign in a small urban pond in Delft, The Netherlands (Cfb), in order to investigate the energy balance during hot summer nights. It has been demonstrated that although waterbodies provide warming to their urban surroundings, only 11% of the released heat consist of sensible heat flux, the rest was associated with longwave radiation (43%) and latent energy (39%). This is important since only sensible heat is related to changes in ambient air temperature, although radiated heat may be absorbed by the surrounding urban context and then reradiated or subsequently lost as sensible heat. The authors also highlight the important role of the preceding day's weather condition on the temperature profile of the water column the following night.

A different approach of tackling the problems associated with the urban climate is the use of full-scale or reduced-scale physical models, among which wind tunnels is the dominant technique. The main advantage of wind tunnels is the almost entire control over the boundary conditions, although this does not apply to the physical models exposed to the external environment. To best of the authors' knowledge, the only wind tunnel study that has considered the performance of water bodies in relation to an urban context is that of Narita (1992), which is written in Japanese and focuses on the water vapour distribution around a building array. Hence, although some wind tunnel research has been carried out on evaporation (Chu et al., 2010; Raimundo et al., 2014), there is little scientific understanding regarding the thermal impact of blue spaces on the urban thermal environment.

In a recent study, Syafii et al. (2016) employed an outdoor reduced-scaled experimental model of a city block (Kanda et al., 2006), in Saitama, Japan (Cfa), in order to study in detail the thermal effects of a typical water pond. This physically idealised model (consisting of a regular array of concrete blocks) was used to isolate distinct parameters to evaluate their influence on the waterbody's cooling potential. Despite the cooling effect of almost 2.5 °C during the warmest part of the day, they also found that during the night urban blue spaces could be warmer than their urban context. Using the same outdoor physical model, Syafii et al. (2017) investigated how different configurations and sizes affect a pond's ability for urban thermal regulation. Results showed that the larger the pond is, the larger the cooling effect in the nearby urban area. As far as orientation is concerned, ponds parallel to the dominant wind direction appeared to be more effective with a mean air temperature reduction of approximately 1.5 °C at a height of 30 cm above the water, corresponding to the down-scaled pedestrian level. Finally, Syafii et al. (2017) also addressed the possible negative effects of the increased humidity, which could be a detriment to thermal comfort.

Although the above-mentioned experimental studies tried to overcome the site-specific nature of field observations, further research should be carried out to produce more general design guidelines that are not dependent on the heterogeneity of the urban context. In fact, studies based on observational data are hard to compare since they are highly site-specific and representative only of the studied waterbody's characteristics, e.g. size, depth, shape, orientation etc. Furthermore, it is noteworthy that the vast majority of the studies were conducted in humid subtropical climates (Cfa), mainly in Asiatic regions. Hence, it is advisable that further observational studies are conducted in other climates and regions around the world.

5. Remote sensing

Remote sensing belongs to the observational techniques and involves the acquirement of useful information regarding an object without being in physical contact with it. In this context, remote sensing typically refers to the gathering of luminosity data via satellite-based sensors, which can be used to infer surface temperatures. This technique has gained popularity over recent years as more data becomes publicly available. Due to the strong correlation between Land Surface Temperatures (LST) and near-surface air temperatures (Cristóbal et al., 2008), remote sensing images have been extensively used to quantify the UHI since they provide boundary conditions to run numerical models and can be used to foster landscape design strategies. Compared to data retrieved from site measurements, remote sensing provides detailed land cover information as well as LST of a broader area at a specific time of the day. Several imaging instruments onboard satellites have been used by researchers to obtain data related to the cooling potential of green and blue spaces. Namely, Advanced Spaceborne Thermal Emission and Reflection Radiometer (ASTER) (Kato and Yamaguchi, 2005; Liu and Weng, 2008), Moderate Resolution Imaging Spectroradiometer (MODIS) (Wang et al., 2007), Landsat Thematic Mapper (TM) and Landsat Enhanced Thematic Mapper Plus (ETM+) (Chen et al., 2006; Li et al., 2011; Weng et al., 2004) are among the well-known satellite data sources.

Nonetheless, remote sensing models should be treated with caution since they rely only on sensible heat and for a given moment in time; the conversion of received shortwave solar radiation into latent heat through the mechanism of evapotranspiration is neglected (Gunawardena et al., 2017; Sun and Chen, 2012, Völker et al., 2013). Furthermore, remote sensing tends to overestimate daytime temperatures and underestimate nocturnal ones (Mohan et al., 2013). This can be attributed to the fact that satellite-derived data tend to over-represent the contribution of the tops of trees and building roofs, which typically have low thermal inertia, and thus represents urban areas as being more thermally responsive than they really are. This, in turn, accentuates the diurnal temperature range of urban areas, i.e. higher surface temperatures during the day and lower surface temperature during the night (Roth et al., 2007). In addition, the remote sensor's field of view, meaning the angle from which the sensor 'sees' the surface, may be unable to capture the effects of vertical shading, especially in high-rise buildings, and thus lead to an underestimation of the surface temperatures for these structures. Uncertainties also hide behind the estimation of emissivity and the different methods used for that purpose (Gillespie,

2014), e.g. temperature and emissivity separation algorithm (Gillespie et al., 1996), reference channel approach (Kahle et al., 1980) etc.

One of the first studies that tried to assess the impact of waterbodies found that wetlands can provide cooling during the warm months and warming during the winter (Shudo et al., 1997). Cao et al. (2010) in an effort to relate the Park Cooling Intensity (PCI), meaning the LST difference between the centre and the surroundings of a park, to several park characteristics in Nagoya, Japan (Cfa), employed ASTER satellite images. Results suggest that regularly shaped parks have a higher cooling potential (°C), i.e. the difference between the average LST inside the park and the average LST of an urban area located 500 m outside the park, given that the shape factor, meaning the previously mentioned land shape index (LSI), is positively correlated to the formation of PCI. However, the authors found no significant relationship between the bodies of water inside the parks and the mitigation of the UHI. According to Cao et al. (2010), that outcome may derive from the small sample of parks, namely 9 out of 18 parks, which contained a pond or lake. These results were confirmed by a later study of 197 waterbodies in Beijing, China (Dwa) suggesting that the smaller LSI, i.e. round or/and square geometries, of a blue space the higher the cooling impact on the urban environment (Sun and Chen, 2012). This can be attributed to the greater fetch of regularly shaped bodies that lead to better atmospheric advection. However, the authors did not account for the wind direction in their analysis; in locations with varying wind direction, a regularly shaped waterbody may be more beneficial, whereas in a location where the wind direction is constant more elongated shapes aligned with the wind would seem to be more appropriate. Another reason is that such regular geometries can amplify humidity and temperature gradients between the blue space and the surrounding urban context. Furthermore, Sun and Chen (2012) found that although the area of a waterbody was significantly correlated with the Urban Cooling Intensity (UCI) (°C/hm), the larger waterbodies provide a less efficient (°C/hm/ha) cooling effect. This suggests that several smaller blue spaces present better spatial distribution but with a lower cooling intensity compared to a single waterbody of the same total size (Sun and Chen, 2012). Finally, the authors also highlighted that densely built urban areas tend to increase both cooling efficiency and intensity. Qualitatively, similar outcomes were obtained from a precedent study in Beijing (Sun et al., 2012). Other studies in Beijing showed that waterbodies' contribution is most evident at a distance of less than 300 m (Hou et al., 2012; Hou et al., 2009). Interestingly, Chun and Guhathakurta (2017) tried to estimate the thermal impact of various land-use types on both the daytime and night-time land surface temperatures, using regression analysis. Results highlighted that waterbodies (both static and dynamic) provide a cooling effect during the day but worsen the UHI intensity during the night.

In recent years, there has been an increasing number of studies that use remote sensing images to assess the UHI and the contribution of waterbodies. The vast majority of them are conducted in Asiatic regions. A recent example can be found in the work of Cai et al. (2018) who indicated that waterbodies in Chongqing, China (Cfa) show a cooling potential that is strongly related to the surrounding urban form and the surface temperatures within a distance <500 m. Luo and Li (2014) also studied the contribution of waterbodies and vegetation in the city of Chongqing using Landsat 5 Thematic Mapper (TM) images. Further examples of recent studies are Chowdhury et al. (2017), Dai et al. (2019), Du et al. (2016), He et al. (2019b), Khalaf (2018) and Xue et al. (2019). Although relatively fewer in number, studies using remote sensing to study the UHI in Europe, suggest that waterbodies can mitigate urban air temperatures from 1 °C up to 10 °C, e.g. in Oláh (2012) (Budapest, Dfb) and Schwarz et al. (2012) (Leipzig, Cfb). Waterbodies were found to be the main cooling mechanism for an urban area in Toronto, Canada (Dfb) (Rinner and Hussain, 2011).

6. Numerical modelling

Numerical solutions to urban climate problems can be achieved by using different software tools, which are mainly based on CFD and/or Energy Balance Models. Simulations with CFD are a powerful alternative to observational and experimental studies as it may overcome some inherent limitations of the latter. Namely, the use of CFD can provide useful information across the entire studied area, whereas the other methods only perform a limited amount of point measurements in space. Additionally, simulations are run under fully controlled conditions, with the opportunity to isolate different

parameters and perform comparative analyses based on different scenarios. Numerical simulations also lack similarity constraints, i.e. the difficulty to ensure that the results of an experiment do not depend on the scale of the model (Blocken, 2015; Robinson, 2012). In comparison with Energy Balance Models, CFD models may include humidity and pollutants, provide a successful coupling between temperature and velocity fields, and simulate in detail flow fields at finer scales than is typical for observations, e.g. building or human scale. (Toparlar et al., 2017). The main disadvantages are the high computational cost, although this has decreased dramatically in recent years due to the increase in standard PC computing power, the requirements of a high-resolution representation of the studied area and the need for information regarding boundary layer conditions for every single flow involved in the process (Blocken, 2015; Mirzaei and Haghighat, 2010). It should be noted, however, that the latter would also be required to fully analyse an observational study.

Although the inclusion of numerical modelling in the assessment of the thermal effects of blue spaces began at the end of the 20th century, the method has only gained notoriety during the last few years. A well-defined simulation is vital in order to obtain accurate results, as such, researchers should pay attention to the geometrical representation of the model, the structure of the computational domain, the selection of solution methods, and the interpretation of the results (Blocken, 2015).

Nagarajan et al. (2004) simulated two days in June near the subarctic region of the Mackenzie River Basin (Dfc) in Canada in an effort to assess how thermal effects of small lakes influence vertical transport within the atmospheric boundary layer. Simulated results were compared against aircraft measurements for the selected times of the day. Results for the 5-hour simulation between 19:00 and midnight showed up to 9% decrease in the sensible heat flux and up to 82% increase in the latent heat flux compared to the base case scenario without lakes. It is worth mentioning that the increase in the latent heat flux was larger for the day of stronger wind speeds and colder lake surface temperatures, meaning that the surface-to-air temperature gradient was greater and, thus, a stable layer was formed restricting the vertical transport of humid parcels of air. Furthermore, apparent heating was observed up to the first 150 m from the water's surface, while a decrease in ambient temperature occurred above that height. However, a moisture burden to the PBL is only apparent between the lowest atmospheric layers (50 – 150 m). This was one of the first studies that mentioned the relationship between water-atmosphere flux and the stability of the surface layer, as well as the available moisture content.

A more sophisticated approach was developed by Robitu et al. (2004), in which they proposed a coupling methodology between the thermo-radiative tool SOLENE (Miguet and Groleau, 2007)) and the commercial CFD software ANSYS Fluent (2015) in an effort to account for the thermal effects of waterbodies on building energy consumption. Results showed that at a distance of approximately 30 m even small ponds (4 m²) could lower the ambient temperature by almost 1 °C at 1 m height. Based on the same coupling procedure, Robitu et al. (2006) proposed an improved model to investigate the influence of blue and green spaces on the urban thermal environment under summer conditions, showing an overall beneficial impact on both outdoor thermal comfort and surface temperature reductions. However, one should consider that it is impossible to assign the effects to either green or blue spaces when they are included simultaneously in the study. Another dynamic model for simulating water ponds or masses of water was developed by de la Flor and Domínguez (2004). These authors assumed a well-mixed waterbody with a constant average temperature, arguing that in relatively shallow waterbodies (<1 m), vertical temperature gradients are negligible.

In an effort to examine the influence of blue space distribution and size on the urban environment, Theeuwes et al. (2013) simulated an idealised circular city (Cfb) using the Weather Research and Forecasting (WRF) model, a mesoscale simulation tool, which was coupled with the land surface model unified-NOAH (Chen et al., 2011) and a single-layer Urban Canopy Model (Tewari et al., 2007). In contrast to previous studies, a full diurnal approach was adopted in order to study how the thermal effects of waterbodies differ between day and night. For this reason, a single urban canopy layer was preferred against a slab model since it provides an accurate representation of the urban boundary layer during the night-time when thermal radiation is trapped within the urban context; such an approach is recommended for mesoscale studies (Kusaka et al., 2001). In the case of a slab model, which treats the domain as a flat surface, all the roughness elements have the same temperature and hence there is a

tendency to overestimate the night-time cooling rate since the heat storage of high thermal capacity materials is omitted. In agreement with Sun and Chen (2012), the results suggest that larger blue spaces present a higher littoral and downwind cooling, compared to several smaller waterbodies with a similar total surface area, although the latter can influence a broader city area. What is more, the authors highlighted that blue spaces can potentially act as a thermal buffer when their surface temperature is higher than the ambient temperature of their urban surroundings, slowing the cooling of urban areas. Namely, the introduction of a lake with 15 °C constant water temperature can reach a maximum cooling effect of up to 1.8 °C at 10:00 but can also lead to a nocturnal warming effect of up to 1 °C, which reaches its maximum at 06:00. With an increased water temperature (20 °C), this warming can be as high as 3.5 °C at 06:00. This warming of the urban surroundings can be attributed to the relatively increased water surface temperature during the night due to the combined effect of limited evaporative flux and water's high thermal capacity. As previously said, during the early afternoon convective instability reaches its maximum and so does the evaporative flux, whilst during the evening and night, the atmosphere becomes more stable, inhibiting vertical transport. Therefore, the additional evaporative cooling leads to the saturation of air above the water surface and further decreasing vertical transport, and thus to decreased evaporative flux. This, in turn, seems to limit horizontal advection and prevent the breaking up of the overlying stabilised atmosphere. Nevertheless, as mentioned in Gunawardena et al. (2017), if a waterbody-breeze system is hypothesised – similar to park-breezes created by green areas, a reversed horizontal advection current could be formed during the night, transporting cooler air towards the body and humid and warmer air to the urban surroundings. In general, warming is more apparent during the end of the summer when water's temperature peaks due to the accumulated heat. Therefore, when the diurnal cycle of water's thermal exchanges is accounted for, waterbodies can provide warming when least needed (night-time, under severe heat waves) and thus lead to exacerbated thermal comfort conditions (Gunawardena et al., 2017).

Theeuwes et al. (2013) also studied the atmospheric vertical structure above the lakes. During the morning, apparent cooling was observed within the first 500 m and warming at higher altitudes. In the afternoon, when the vertical transport is stronger, cooling was found at all altitudes. The warming effect was obvious only at lower altitude during the night. Although the significant contribution of available surface water to its urban thermal environment was pointed out, several parameters were not taken into consideration, i.e. waterbody area, distance from the urban core and LSI (Sun and Chen, 2012). This offers the prospect of conducting further research on this area.

Following a similar coupling procedure, Morris et al. (2016) used the mesoscale WRF model to assess the mitigating potential of green and blue spaces in the city of Putrajaya in Malaysia (Af). The simulated outputs were validated against in-situ measurements. The methodology employed the study of different urban fractions by replacing a part of waterbodies and green spaces with impervious urban residential surfaces. With regard to blue spaces, 12% of the city's water coverage was replaced with high-density urban materials, while keeping the vegetation proportion constant, in this way, the authors were able to quantify the contribution of waterbodies. Results are in agreement with Theeuwes et al. (2013) as an undesirable warming effect was observed in the early hours and during the night. More specifically, this became obvious as the decreased water coverage led to a cooling effect during the night-time (01:00 – 10:00) and an average increase of UHI intensity (between 11:00 – 16:00) of 0.3 °C. All air temperatures were calculated at a 2 m height. Žuvela-Aloise et al. (2016) concluded that waterbodies (including water ponds, lakes and rivers) can warm or cool the urban climate depending on water temperature, time of the day, the surrounding built environment and the local climatic conditions. Their research employed the urban climate model MUKLIMO_3 that uses the Reynolds Averaged Navier Stokes (RANS) model for calculating turbulence. An idealised and a real case model of the city of Vienna, Austria (Cfb) were simulated, with the latter being validated against observational data of more than 10 years of measurements from 7 weather stations. Their results indicated that the assessment of the cooling potential of blue (and green) infrastructure is very difficult to use to inform a general urban planning strategy, since different effects may happen even in different locations within the cities, let alone different climates.

A growing number of studies are now utilising more detailed simulations within coupled model frameworks. However, due to the complexities and the significant amount of input data required by the

usual commercial simulation tools, there are huge discrepancies between the different applications. Hence, the task of classifying and categorising the existing literature in an effort to identify patterns and scientific gaps has become very difficult. For example, in the study of Taleghani et al. (2014), three scenarios of possible mitigation techniques were assessed using the three-dimensional microclimate model ENVI-met, which applies basic thermodynamics and fundamental laws of fluid dynamics in order to assess interactions between surfaces, vegetation and air in the urban environment (Bruse and Fleer, 1998). Although the results suggest that the presence of waterbodies in the campus of Portland State University (Csb) can lead to a cooling effect of approximately 1 °C, the authors provided little detail of the blue space characteristics and the simulation set-up, namely the area input file and the configuration file. The first provides useful information regarding the soil type, vegetation and building characteristics while the latter contains crucial initial settings, e.g. weather input data. The precision of the calculated results is dependent on the input parameters and the initial boundary conditions (Maleki et al., 2014). In a recent study conducted in West Kensington, London (Cfb) (O'Malley et al., 2015) the authors tried to assess the resilience of different UHI mitigation techniques making use of ENVI-met and including urban waterbodies, as well as their cooling potential. Results showed that the inclusion of urban blue spaces could not ameliorate the UHI although a mean air temperature decrease of 0.1 °C was found. However, according to the published details, simulations were run only for ten hours during the daytime (between 10:00 and 20:00); hence, there was not enough time for the simulation to reach a steady-state condition. In addition, the paper lacks a description of the simulation set-up parameters and the waterbodies' characteristics. In a similar climate (Toulouse, France – Cfb), Martins et al. (2016) used ENVI-met to assess the contribution of different strategies on the mitigation of the summertime UHI. Although some simulation details were provided, the authors offered little discussion regarding the water ponds' characteristics, such as depth, area etc. Their results indicated a positive cooling effect of waterbodies, ranging from a maximum reduction of 6 °C at 12:00 and 2 °C at 24:00. Similarly, Jin et al. (2017) investigated the influence of different water pond configuration, i.e. dispersed or scattered, in a residential district in northeast China (Harbin City – Dwa), deploying the simulation tool ENVI-met but simulating only for seven hours during the day (09:00 to 16:00). Another example of a numerical modelling study that provided very few details of the simulation set-up is the one by Amor et al. (2015), who investigated the relative contribution of the addition of two small ponds on thermal comfort conditions in an urban square in Sétif, Algeria (Csa). In addition, the authors considered only the evaporative area of the waterbodies as the influencing parameter, concluding that water ponds are related to a higher extent with the addition of humidity rather than affecting ambient temperature. This is in agreement with the findings of the observation study of Solcerova et al. (2019).

Tominaga et al. (2015) conducted a numerical study (Hadano City, Japan – Cfa) to evaluate the simulation accuracy of Fluent on calculating the evaporative cooling effect of small water ponds, the mechanism of vapour transport around building blocks and how the water surface can mitigate the thermal environment in an urban residential district. The validation was made against two previous wind tunnel experiments and an observational study carried out by the authors. The computational domain was built following the body-fitted technique proposed by van Hooff and Blocken (2010a, 2010b), which uses prismatic or hexahedral cells and allows full control on grid resolution and quality. The simulations were coupled with the P-1 radiation model and the shell-conduction model for heat exchange through building walls and with the ground (Fluent, 2015). The authors also modelled evaporation from the water surface and water vapour transport; both were validated against observational data. Results showed that CFD simulations tend to overestimate vapour pressure ratio above the water surface, while the opposite happens within the building arrays, meaning that the turbulent diffusion downwind is underestimated. This has been already mentioned by previous studies and has been attributed to the inability of RANS models to appropriately estimate scalar transport properties (Tominaga and Stathopoulos, 2011). Further analysis pointed out a cooling effect of up to 2 °C, which is mainly dependent on wind direction, building configuration and water surface characteristics. If there is no obstruction by the surrounding built environment, air temperature decrease can be observed over 100 m downwind (wind speed: 3 m/s, height: 10 m). At this point, it should be mentioned that the authors did not account for the existence of green spaces or anthropogenic heat release, isolating the contribution of waterbodies to the thermal environment. Additionally, the heat storage of buildings and other urban surfaces was also omitted, something that could exacerbate heat

stress during the night, when the most intensive UHI is observed since longwave radiation is emitted back to the urban environment. In fact, the temporal variations of waterbodies' cooling effectiveness are highly documented (Theeuwes et al., 2013). Nonetheless, the analysis was carried out only at 15:00. Furthermore, waterbody characteristics, such as pond's depth, stratification and surface area, were not presented in the paper. Again, this approach can lead to serious misunderstandings in terms of blue spaces' effect on the urban thermal environment because it only provides case-specific conclusions that cannot be included in a general framework.

In a more recent study, Zhao and Fong (2017a, 2017b) used ENVI-met to assess the cooling potential of waterbodies with different area coverage ratio in an idealised city, which was based on the typical urban form of Hong Kong (Cfa). In their first study, the ENVI-met model was validated against in-situ measurements using the City University of Hong Kong as a representative urban environment. Based on the simulation settings of their first study, the authors simulated a typical urban district, with 44% of the area being buildings, and concluded that if the blue spaces covered more than 34% of the domain, cooling effects can be generated. On the contrary, if urban waterbodies are employed across a smaller percentage area, then the air temperature reductions, which range between 0.7 and 1.5 °C according to different area coverage ratios, are insufficient to compensate for the increased humidity and the consequent exacerbated thermal comfort. However, these results must be interpreted with caution since they imply that the water vapour is staying at street level and not being dissipated as a result of increased vertical transport. In fact, given the previous discussion presented in this paper, one would expect that given the selected time of the day (15:00), the atmosphere would be unstable enhancing vertical motion of fluid particles.

Using the open-source CFD code OpenFOAM, Abbasi et al. (2018) studied the effects of a small and shallow lake on the airflow and heat exchanges in the PBL over an arid region in Ghana (Aw). In their model, unsteady RANS equations were solved along with the realisable k-ε turbulence model. The generation of turbulent kinetic energy by buoyancy and the effects of atmospheric stability were also taken into consideration. The former was added in the equations of turbulent kinetic energy (k) and the dissipation rate of kinetic energy (ε), while the latter was implemented in the time-dependent non-uniform heat flux on the surface. Results showed that under unstable conditions the flow velocity experiences sharp changes when passes from land to water surfaces, mainly because of the decrease in surface roughness (from 0.13 m to 0.0001 m), whilst the air temperature changes are negligible. On the contrary, when the atmosphere above the water surface is stable, the flow velocity profile does not present any particular pattern but there are significant changes in the air temperature profiles. Further research needs to examine more closely the links between atmospheric stability conditions and the thermal effects of waterbodies on their urban surroundings.

7. Discussion

The assessment of the thermal effects of blue space on the urban climate involves different tools, including field measurements, reduced-scale experimental studies, remote sensing and numerical simulation models. Apart from the different approach that each tool offers, the climatic conditions, urban morphology, waterbody geometry and parameters included can induce great discrepancies, making it challenging to compare results from different studies.

7.1 The impact of water stratification

The assumption of a well-mixed waterbody and consequently a constant water temperature is quite typical amongst the existing literature. This is mainly because most of the studies assess the impact of relatively shallow and small bodies of water, e.g. in de la Flor and Domínguez (2004), Theeuwes et al. (2013) and Tominaga et al. (2015). However, as already said, recent studies have proven that even shallow static blue spaces may exhibit long term and repeated stratification (Abbasi et al., 2016; Abis and Mara, 2006; Song et al., 2013). Generally speaking, only bodies <1 m deep can be described as isothermal, meaning that the whole column of water participates in the thermal exchanges between the water and the immediate environment above (Song et al., 2013). In fact, small shallow blue spaces are

becoming more commonplace as part of Sustainable Drainage Systems (SuDS) as largescale urban development plans receive growing attention (Gunawardena et al., 2017). Hence, the inclusion of stratification and the effect of different depths of waterbodies presents an opportunity for further research in the interaction between waterbodies and the urban climate.

7.2 The effect atmospheric moisture and stability

The vast majority of the studies reviewed tend to focus only on the daytime evaporative cooling effect of blue spaces. However, there is evidence that even this daytime cooling potential is somewhat misleading. It has been shown that in some instances the increased humidity due to evaporation can negate or attenuate the thermal relief from sensible cooling (Theeuwes et al., 2013; Zhao and Fong, 2017a). In addition, emphasis is usually put on the spatial distribution of the cooling effect of waterbodies (Tominaga et al., 2015). The greatest temperature reductions are found downwind, with obstructions (placement of buildings and trees), wind direction and water surface area being the most important variables. However, in order to better understand how blue spaces influence the UHI_{UBL} and the local microclimate, conducting research into the vertical transport and temperature structure of the atmosphere above the water is of great importance. This includes the effects of atmospheric stability conditions on the temperature, velocity and turbulence profiles above the waterbody, which can actually alter the evaporation from the open water surface (Abbasi et al., 2017a). Nonetheless, only a few studies focused on the vertical distribution of waterbodies' thermal effects (Nagarajan et al., 2004; Theeuwes et al., 2013), meaning that effects such as the hypothesised cyclic waterbody breeze system (Gunawardena et al., 2017) and its impacts on the surrounding urban context have not been sufficiently explored. Additionally, far less attention has been provided to the study of atmospheric moisture inside the UCL (with and without the presence of a waterbody) despite its significant role on evaporative cooling (Oke et al., 2017; Yang et al., 2020).

7.3 Diurnal and seasonal variations of the cooling effect

One common finding, related to the structure of the atmospheric layers above a water surface, is that the cooling effect of blue spaces varies, depending on the time of the day and season. These variations can be explained by the diurnal and annual variations in the evaporative flux. Considering the diurnal cycle (Figure 6), during the early morning as the Sun warms the water surface, convective vertical transport is induced and the atmospheric water vapour content increases. However, during the early afternoon, the enhanced water-to-air temperature gradient gives rise to buoyancy-driven transport of warmer and less dense air into the UBL. This means that colder, denser and less saturated air moves to lower altitudes. At this point of the day convective instability, evaporative flux and water surface temperature reach their highest point. As the day progresses the decreased air temperature leads to a more stabilised atmosphere and thus reduced vertical transport, meaning that water evaporation will now reduce the water-to-vapour pressure deficit and thus restrict evaporative flux (Oke, 1987). This, in combination with the differential cooling rates of the waterbody and the surrounding urban surfaces, which cool faster, reduces night-time advection and may lead to a warming effect, this is more apparent when water reaches its highest temperature towards the end of the summer. It is possible, therefore, that waterbodies can also moderate ambient temperatures and temporal variations by acting as a thermal buffer due to their increased thermal inertia.

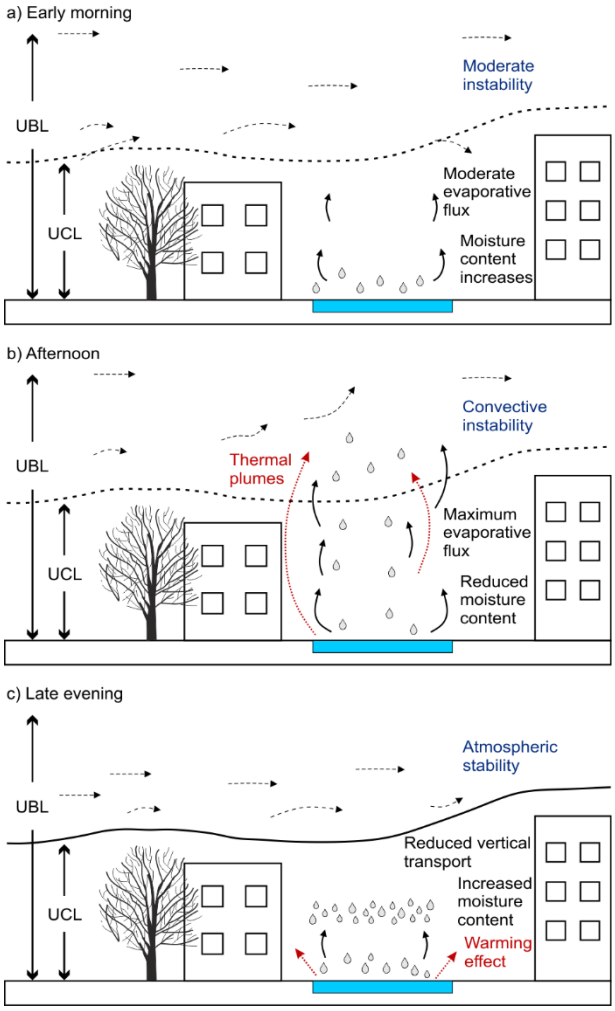

Figure 6: Diurnal evaporative cycle of urban blue space.

7.4 Warming effect

It is somewhat surprising that there are only a few studies underlining the warming effect of waterbodies. In particular, Theeuwes et al. (2013) noted that a waterbody of 15 °C water temperature was warmer than its surroundings between 04:00 and 08:00, with a maximum warming effect of 0.7-1 °C at 06:00. When a water temperature of 20 °C was considered, the air temperature close to the waterbody was found 3.5 °C higher than the case without it at 06:00. In a study conducted in similar climate (Cfb), Žuvela-Aloise et al. (2016) found that a waterbody of 23 °C can lead to a warming effect >0.1 °C at 04:00. Nonetheless, when the blue space was simulated with an 18 °C temperature, it provided cooling throughout the day (14:00, 22:00 & 04:00). The reason for these discrepancies may be the different weather boundary conditions of the two models: in the first study air temperature varied between 18-25 °C whilst in the latter air temperature was set to 25 °C. The observational studies of Heusinkveld et al. (2014), Solcerova et al. (2019) and Steeneveld et al. (2014) confirmed qualitatively these results by studying a similar temperate oceanic climate (Cfb). In addition, Solcerova et al. (2019) highlighted the need to study in more detail the thermal behaviour of waterbodies during night-time with respect to their energy balance and temperature structure since, it was shown that, only one-tenth of the total heat released directly influences air temperature. Other numerical modelling studies conducted in temperate oceanic climate (Cfb) did not observe a warming effect during the evening (until 20:00) or night (24:00) (Martins et al., 2016; O'Malley et al., 2015). These qualitative discrepancies may be attributed to different simulation approaches (methodology, set-up parameters etc.) and the fact that different influencing parameters were accounted for, such as the waterbody's size, depth and distribution within the urban context.

7.5 The limitations of remote sensing studies

As already discussed, remote sensing studies should be treated with caution since they do not account for the latent heat of vaporisation, which has been shown to be a large proportion of the heat flux, and they mainly focus on a certain instant in time. Hence, it is not surprising that the warming effect has not been reported in the majority of the remote sensing studies. As a unique example, Chun and Guhathakurta (2017) have shown that when LST data from both day and night are included, the intensification of the UHI by urban blue spaces during the night is evident. Numerous remote sensing studies have tried to assess the UHI and found that waterbodies are by far the coolest element with the urban context. Based on the reviewed studies the average cooling potential of waterbodies was 1.9 °C, 2.4 °C and 5.3 °C according to numerical modelling, observational and remote sensing studies, respectively. Thus, the current evidence implies that remote sensing tends to overestimate the cooling capacity of urban waterbodies. Of course, the reader should bear in mind that the numbers provided above regarding the cooling effect of blue spaces are just a rough estimation in order to identify patterns within the different methods. In fact, more case studies need to be developed in order to provide a valid classification and interpretation of the thermal behaviour of urban blue spaces.

7.6 Blue space geometry and urban form

Despite the above-mentioned drawbacks, when a great number of waterbodies of different shapes, depths and sizes are assessed, the use of remote sensing can lead to useful qualitative conclusions to assist urban design and planning. A notable example is provided by the study of Sun and Chen (2012) who assessed the cooling effectiveness of nearly two hundred waterbodies on the urban environment in relation to several landscape descriptors. Here, the cooling intensity (°C/hm) was positively related to waterbody area and built-up proportion, and negatively related to the distance from the city centre and land shape index (LSI). The latter was confirmed by an observational study carried out in similar climate (Cfa) suggesting that the smaller the LSI (or the rounder the waterbody's shape) the higher its cooling intensity (Li and Yu, 2014). In apparent contradiction, Xue et al. (2019) found a positive correlation between the LSI and the cooling potential of waterbodies, however when considering the cooling efficiency of the waterbodies a smaller negative correlation was indicated. The positive relationship between the size and the cooling effect was also assessed in the experimental study of Syafii et al. (2017). The authors also highlighted that ponds can provide more effective evaporative cooling when they are placed parallel to the prevailing wind. At this point, it could conceivably be hypothesised that in locations with varying wind directions, a more regularly shaped waterbody (a LSI closer to unity) may provide more consistent cooling intensity, whereas in locations where the wind direction is constant more elongated shapes aligned with the prevailing wind would provide greater cooling intensity due to increased fetch. In the analysis presented by Xue et al. (2019) wind direction was not considered, as such the discrepancy between their conclusions and those of other studies could be the result of the irregular waterbodies being more favourably aligned to the wind direction at the time of observation. It should also be noted that any upwind natural or artificial windbreak can potentially reduce wind speeds and increase turbulent mixing downwind, resulting in a decreased humidity gradient and thus limited evaporative flux (Gross, 2017; Hipsey and Sivapalan, 2003). Finally, it has become apparent that there is a lack of studies dealing with the effects of the urban and the properties of the urban surfaces on the cooling potential of blue space (Hathway and Sharples, 2012).

7.7 Methods and underlying climate

The vast majority of the reviewed studies were conducted in humid subtropical climates (Cfa), mainly in Asiatic regions. Some observational studies from these areas, including both field campaigns and reduced-scale models, found blue spaces to be warmer than their urban context during the night (18:00 – 06:00) or early morning (06:00 – 10:00), additionally that the water surface area and increased humidity play important roles in the overall effect on the surrounding thermal environment (Huang et al., 2008b; Syafii et al., 2017; Syafii et al., 2016; Yang and Zhao, 2016). However, other field studies conducted in similar climate zones did not reveal these negative impacts of static waterbodies (Chen et al., 2009; Ishii et al., 1991; Nishimura et al., 1998; Xu et al., 2010). A possible explanation may be the

selected time (usually daytime), or the season, in which the observations were made, the inclusion of both green and blue spaces, and disparate weather conditions. Interestingly, only one study employing numerical modelling found a negative effect of blue spaces in a humid subtropical climate, that is the implementation of a waterbody with an area coverage smaller than 34% would exacerbate thermal comfort at pedestrian level (Zhao and Fong, 2017a, 2017b). This was attributed to the fact that air temperature drop could not counterbalance the increased humidity levels. This implies that moisture remained at street level and was not transported to higher altitudes despite the expected convective instability of the atmosphere at the selected time of the day (15:00).

There is a wide discrepancy between the climates in which the different studies are conducted. Out of 13 field measurement studies, the vast majority have been carried out in humid subtropical climates (~69%), followed by temperate oceanic (~23%) and hot-summer Mediterranean (~8%). Therefore, considering the importance of field measurements on validating simulation results and providing input parameters there is an urgent need for more field measurements across different climates. However, it is significant to note that local urbanisation affects urban static waterbodies, increasing their water temperature in relation to their rural counterparts. This 'urban hot-tub effect' peaks during summer with a recorded mean water temperature difference between urban and rural ponds (ponds in different provinces of Belgium – Cfb) of about 3 °C (Brans et al., 2018). Since the heat lost by an urban waterbody has been shown to be ~43% longwave radiation (Solcerova et al., 2019), the interplay between a water surface and the surrounding urban context and the resultant radiant environment is a crucial consideration. This imposes greater complexity on simulation studies, which tend to rely on observational data from urban environments with different morphologies and urban densities. In terms of numerical modelling, although wider spread, the majority of them are conducted for humid subtropical (~29%) and temperate oceanic climates (~35%). In summary, studies employing simulations or observations account for about 59% of the total studies that have been covered in this review, with remote sensing being by far the most popular approach (~41%).

The increased popularity of remote sensing studies can be attributed to the ease of obtaining remote sensing data compared to the more demanding field observations. The latter is usually more time consuming and requires appropriate equipment, which can be costly and potentially complex to use, as well as good weather conditions to conduct the measurements. Given the growth in the number of both remote sensing and numerical studies, future studies employing observations and more than one technique are therefore recommended, as they can allow comparative analysis. Supplementary material of the reviewed literature can be accessed online, containing summary tables for observational (Table 3), remote sensing (Table 4) and numerical modelling studies (Table 5).

8. Summary

In view of the current trend of increasing urbanisation and the need to regulate the thermal urban environment, this paper has considered the contribution of blue spaces by reviewing the existing literature.

Despite the insight provided by the existing range of studies, there seem to be significant discrepancies between the methods, the parameters considered and the background climate in which each study is carried out. Observational studies are mainly conducted during the daytime while the vast majority (~69%) of them are in humid subtropical climates. Remote sensing studies focus only on a certain instant in time and tend to overestimate the waterbodies' cooling capacity due to a lack of nocturnal measurements and the inability to capture the latent heat flux. On the other hand, studies that employ numerical modelling, although more geographically distributed, lack a consistent approach. This, in combination with their limited number compared to other UHI mitigation strategies, calls for further research contributions in order to provide a valid classification of the overall influence of blue spaces on the urban climate. Additionally, it is recommended that future studies should employ more than one technique in order to facilitate comparative analysis which is currently lacking. Lastly, a greater variety of urban locations should be investigated.

The meta-analysis presented in this study was designed particularly to determine the thermal effects of static blue spaces on the urban climate. However, investigation of the literature has shown that there is a distinct knowledge gap regarding the physical interpretation of waterbodies contribution. For instance, there is a need to further study the vertical transport and temperature structure to at least twice the height of buildings above a body of water in order to assess whether it acts as a cooling agent, via the evaporation of water and the promotion of vertical transport of air, or as thermal buffer storing heat to be radiated later further, exacerbating the heat island effect and worsening environmental conditions via increased humidity and radiant temperatures. Currently, the interplay between those two inter-related effects and how their relationship varies according to the waterbody's size, depth, shape and location, is unclear. There is also a current lack of information about the diurnal and seasonal variability of the structures and processes. The evidence from this study suggests that in order to inform urban planning and design guidelines in a holistic way, it is advisable to extend the research of urban blue space to include the night-time when the UHI is most apparent and the risk of heat stress is the greatest. Furthermore, the influence of atmospheric stability conditions on evaporation and vertical transport of heat above a waterbody needs to be investigated further.

Several researchers have suggested that the implementation of several smaller blue spaces within an urban context can provide a more dispersed cooling in comparison to a single larger waterbody that in contrast can provide a greater but localised cooling effect. Nonetheless, it is not yet clear how the proportion and geometry of the waterbody as well as of the surrounding built-up area and the distance from it, alter the overall thermal effect. For instance, there is evidence that the comfort achieved by sensible cooling may not always compensate for the increased water vapour content. If this is the case, the prevailing wind conditions can play an important role. Despite the general belief that rounder blue spaces present better cooling potential, this would only be the case when the local climate comes with random wind directions. In contrast, a more elongated waterbody might be more efficient, due to the greater fetch, with a narrower range of wind directions. Further research is therefore needed to establish the relationships between the urban form and the thermal behaviour of blue spaces. This can then lead to studies that promote comprehensive design principles regarding the implementation of blue space in the urban core.

References

Abbasi A, Annor FO, van de Giesen N. Investigation of Temperature Dynamics in Small and Shallow Reservoirs, Case Study: Lake Binaba, Upper East Region of Ghana. Water 2016; 8. https://doi.org/10.3390/w8030084.

Abbasi A, Annor FO, van de Giesen N. Effects of atmospheric stability conditions on heat fluxes from small water surfaces in (semi-) arid regions. Hydrological Sciences Journal 2017a; 62: 1422-1439. https://doi.org/10.1080/02626667.2017.1329587.

Abbasi A, Annor FO, van de Giesen N. A framework to simulate small shallow inland water bodies in semi-arid regions. Advances in Water Resources 2017b; 110: 77-96. https://doi.org/10.1016/j.advwatres.2017.09.023.

Abbasi A, Annor FO, van de Giesen N. The effects of small water surfaces on turbulent flow in the atmospheric boundary layer: URANS approach implemented in OpenFOAM. Environmental Modelling & Software 2018; 101: 268-288. https://doi.org/10.1016/j.envsoft.2017.12.013.

Abis KL, Mara D. Temperature measurement and stratification in facultative waste stabilisation ponds in the UK climate. Environ Monit Assess 2006; 114: 35-47. https://doi.org/10.1007/s10661-006-1076-7.

Amor B, Lacheheb DEZ, Bouchahm Y. Improvement of Thermal Comfort Conditions in an Urban Space (Case Study: The Square of Independence, Setif, Algeria). European Journal of Sustainable Development 2015; 4: 407-416. https://doi.org/10.14207/ejsd.2015.v4n2p407.

ANSYS Fluent. Theory guide. Ansys Inc, 2015.

Arnfield AJ. Two decades of urban climate research: a review of turbulence, exchanges of energy and water, and the urban heat island. International Journal of Climatology 2003; 23: 1-26. https://doi.org/10.1002/joc.859.

Barlow JF. Progress in observing and modelling the urban boundary layer. Urban Climate 2014; 10: 216-240. https://doi.org/ 10.1016/j.uclim.2014.03.011.

Berglund L. Thermal acceptability. ASHRAE Transactions 1979; 85(2): 825-834.

Blocken B. Computational Fluid Dynamics for urban physics: Importance, scales, possibilities, limitations and ten tips and tricks towards accurate and reliable simulations. Building and Environment 2015; 91: 219-245. https://doi.org/10.1016/j.buildenv.2015.02.015.

Boehrer B, Schultze M. Stratification of lakes. Reviews of Geophysics 2008; 46. https://doi.org/10.1029/2006rg000210.

Brans KI, Engelen JMT, Souffreau C, De Meester L. Urban hot-tubs: Local urbanization has profound effects on average and extreme temperatures in ponds. Landscape and Urban Planning 2018; 176: 22-29. https://doi.org/10.1016/j.landurbplan.2018.03.013.

Bruse M, Fleer H. Simulating surface–plant–air interactions inside urban environments with a three dimensional numerical model. Environmental Modelling & Software 1998; 13: 373-384. https://doi.org/10.1016/S1364-8152(98)00042-5.

Bünzli D, Schmid HP. The influence of surface texture on regionally aggregated evaporation and energy partitioning. Journal of the Atmospheric Sciences 1998; 55: 961-972. https://doi.org/ 10.1175/1520-0469(1998)055<0961:Tiosto>2.0.Co;2.

Cai Z, Han G, Chen M. Do water bodies play an important role in the relationship between urban form and land surface temperature? Sustainable Cities and Society 2018; 39: 487-498. https://doi.org/10.1016/j.scs.2018.02.033.

Cao X, Onishi A, Chen J, Imura H. Quantifying the cool island intensity of urban parks using ASTER and IKONOS data. Landscape and Urban Planning 2010; 96: 224-231. https://doi.org/10.1016/j.landurbplan.2010.03.008.

Chan SY, Chau CK, Leung TM. On the study of thermal comfort and perceptions of environmental features in urban parks: A structural equation modeling approach. Building and Environment 2017; 122: 171-183. https://doi.org/10.1016/j.buildenv.2017.06.014.

Chen F, Kusaka H, Bornstein R, Ching J, Grimmond CSB, Grossman-Clarke S, et al. The integrated WRF/urban modelling system: development, evaluation, and applications to urban environmental problems. International Journal of Climatology 2011; 31: 273-288. https://doi.org/10.1002/joc.2158.

Chen X-L, Zhao H-M, Li P-X, Yin Z-Y. Remote sensing image-based analysis of the relationship between urban heat island and land use/cover changes. Remote Sensing of Environment 2006; 104: 133-146. https://doi.org/10.1016/j.rse.2005.11.016.

Chen ZL, Zhao LH, Meng QL, Wang CS, Zhai YC, Wang F. Field measurements on microclimate in residential community in Guangzhou, China. Frontiers of Structural and Civil Engineering 2009; 3: 462-468. https://doi.org/10.1007/s11709-009-0066-6.

Chowdhury A, Vanama VSK, Valliappan AL. Examining the Effect of the Physical Characteristics of the Urban Green & Blue Spaces in Heat Mitigation. 38th Asian Conference on Remote Sensing - Space Applications: Touching Human Lives, ACRS 2017, 2017.

Chu C-R, Li M-H, Chen Y-Y, Kuo Y-H. A wind tunnel experiment on the evaporation rate of Class A evaporation pan. Journal of Hydrology 2010; 381: 221-224. https://doi.org/10.1016/j.jhydrol.2009.11.044.

Chun B, Guhathakurta S. Daytime and nighttime urban heat islands statistical models for Atlanta. Environment and Planning B: Urban Analytics and City Science 2017; 44: 308-327. https://doi.org/10.1177/0265813515624685.

Coutts AM, Tapper NJ, Beringer J, Loughnan M, Demuzere M. Watering our cities. Progress in Physical Geography 2012; 37: 2-28. https://doi.org/10.1177/0309133312461032.

Cristóbal J, Ninyerola M, Pons X. Modeling air temperature through a combination of remote sensing and GIS data. Journal of Geophysical Research-Atmospheres 2008; 113. https://doi.org/10.1029/2007JD009318.

Dai Z, Guldmann J-M, Hu Y. Thermal impacts of greenery, water, and impervious structures in Beijing's Olympic area: A spatial regression approach. Ecological Indicators 2019; 97: 77-88. https://doi.org/10.1016/j.ecolind.2018.09.041.

de la Flor FS, Domínguez SA. Modelling microclimate in urban environments and assessing its influence on the performance of surrounding buildings. Energy and Buildings 2004; 36: 403-413. https://doi.org/10.1016/j.enbuild.2004.01.050.

Downing JA. Emerging global role of small lakes and ponds: little things mean a lot. Limnetica 2010; 29: 9-23. https://doi.org/10.23818/limn.29.02.

Driedonks AGM, Tennekes H. Entrainment Effects in the Well-Mixed Atmospheric Boundary-Layer. Boundary-Layer Meteorology 1984; 30: 75-105. https://doi.org/10.1007/Bf00121950.

Du H, Song X, Jiang H, Kan Z, Wang Z, Cai Y. Research on the cooling island effects of water body: A case study of Shanghai, China. Ecological Indicators 2016; 67: 31-38. https://doi.org/10.1016/j.ecolind.2016.02.040.

Gillespie AR. Land Surface Emissivity. In: Njoku EG, editor. Encyclopedia of Remote Sensing. Springer-Verlag, New York, 2014, pp. 303-311. https://doi.org/10.1007/978-0-387-36699-9_77.

Gillespie AR, Matsunaga T, Rokugawa S, Hook SJ. Temperature and emissivity separation from advanced spaceborne thermal emission and reflection radiometer (ASTER) images. Infrared Spaceborne Remote Sensing IV. 2817. International Society for Optics and Photonics, 1996, pp. 82-95. https://doi.org/10.1117/12.255172.

Grimmond CSB, Roth M, Oke TR, Au YC, Best M, Betts R, et al. Climate and More Sustainable Cities: Climate Information for Improved Planning and Management of Cities (Producers/Capabilities Perspective). Procedia Environmental Sciences 2010; 1: 247-274. https://doi.org/10.1016/j.proenv.2010.09.016.

Gross G. Some effects of water bodies on the environment - numerical experiments. Journal of Heat Island Institute International 2017; 12.

Gu R, Montgomery S, Austin TA. Quantifying the effects of stream discharge on summer river temperature. Hydrological Sciences Journal 1998; 43: 885-904. https://doi.org/10.1080/02626669809492185.

Gunawardena KR, Wells MJ, Kershaw T. Utilising green and bluespace to mitigate urban heat island intensity. Sci Total Environ 2017; 584-585: 1040-1055. https://doi.org/10.1016/j.scitotenv.2017.01.158.

Hathway EA, Sharples S. The interaction of rivers and urban form in mitigating the Urban Heat Island effect: A UK case study. Building and Environment 2012; 58: 14-22. https://doi.org/10.1016/j.buildenv.2012.06.013.

He B-J, Zhu J, Zhao D-X, Gou Z-H, Qi J-D, Wang J. Co-benefits approach: Opportunities for implementing sponge city and urban heat island mitigation. Land Use Policy 2019a; 86: 147-157. https://doi.org/10.1016/j.landusepol.2019.05.003.

He B-J, Zhao Z-Q, Shen L-D, Wang H-B, Li L-G. An approach to examining performances of cool/hot sources in mitigating/enhancing land surface temperature under different temperature backgrounds based on landsat 8 image. Sustainable Cities and Society 2019b; 44: 416-427. https://doi.org/10.1016/j.scs.2018.10.049.

He B-J, Ding L, Prasad D. Wind-sensitive urban planning and design: Precinct ventilation performance and its potential for local warming mitigation in an open midrise gridiron precinct. Journal of Building Engineering 2020a; 29: 101145. https://doi.org/ 10.1016/j.jobe.2019.101145.

He B-J, Ding L, Prasad D. Urban ventilation and its potential for local warming mitigation: A field experiment in an open low-rise gridiron precinct. Sustainable Cities and Society 2020b; 55: 102028. https://doi.org/ 10.1016/j.scs.2020.102028.

Heusinkveld BG, Steeneveld GJ, van Hove LWA, Jacobs CMJ, Holtslag AAM. Spatial variability of the Rotterdam urban heat island as influenced by urban land use. Journal of Geophysical Research-Atmospheres 2014; 119: 677-692. https://doi.org/10.1002/2012JD019399.

Hipsey MR, Sivapalan M. Parameterizing the effect of a wind shelter on evaporation from small water bodies. Water Resources Research 2003; 39. https://doi.org/10.1029/2002wr001784.

Holmer B, Eliasson I. Urban–rural vapour pressure differences and their role in the development of urban heat islands. International Journal of Climatology 1999; 19: 989-1009. https://doi.org/ 10.1002/(sici)1097-0088(199907)19:9<989::Aid-joc410>3.0.Co;2-1.

Hou P, Chen Y, Qiao W, Cao G, Jiang W, Li J. Near-surface air temperature retrieval from satellite images and influence by wetlands in urban region. Theoretical and Applied Climatology 2012; 111: 109-118. https://doi.org/10.1007/s00704-012-0629-7.

Hou P, Jiang WG, Cao GZ, Luo AM. Effect of Urban Thermal Characteristics on Wetlands Based on Remote Sensing and GIS. 2009 Joint Urban Remote Sensing Event, Vols 1-3 2009: 1376-+. https://doi.org/10.1109/URS.2009.5137701.

Howard L. The climate of London deduced from meteorological observations made in the metropolis and at various places around it [electronic resource]: Harvey and Darton, 1833.

Huang LM, Li HT, Zhao DH, Zhu JY. A fieldwork study on the diurnal changes of urban microclimate in four types of ground cover and urban heat island of Nanjing, China. Building and Environment 2008a; 43: 7-17. https://doi.org/10.1016/j.buildenv.2006.11.025.

Huang LM, Zhao DH, Wang JZ, Zhu JY, Li JL. Scale impacts of land cover and vegetation corridors on urban thermal behavior in Nanjing, China. Theoretical and Applied Climatology 2008b; 94: 241-257. https://doi.org/10.1007/s00704-007-0359-4.

IPCC. Climate Change 2014: Impacts, Adaptation, and Vulnerability. Part A: Global and Sectoral Aspects. Contribution of Working Group II to the Fifth Assessment Report of the Intergovernmental Panel on Climate Change. Summary for policymakers, Cambridge, United Kingdom and New York, NY, USA, 2014, pp. 1-32.

Ishii A, Iwamoto S, Katayama T, Hayashi T, Shiotsuki Y, Kitayama H, et al. A Comparison of Field Surveys on the Thermal Environment in Urban Areas Surrounding a Large Pond - When Filled and When Drained. Energy and Buildings 1991; 16: 965-971. https://doi.org/10.1016/0378-7788(91)90091-G.

Jin H, Shao T, Zhang R. Effect of water body forms on microclimate of residential district. Energy Procedia 2017; 134: 256-265. https://doi.org/10.1016/j.egypro.2017.09.615.

Kahle AB, Madura DP, Soha JM. Middle infrared multispectral aircraft scanner data: analysis for geological applications. Applied Optics 1980; 19: 2279-2290. https://doi.org/10.1364/AO.19.002279.

Kalff J. Limnology: Inland Water Ecosystems. New Jersey, United States: Prentice Hall, 2002.

Kanda M, Kawai T, Moriwaki R, Narita K, Hagishima A, Sugawara H. Comprehensive outdoor scale model experiments for urban climate (COSMO). Proceedings of the 6th International Conference on Urban Climate, Göteborg, Sweden, 2006, pp. 12-16.

Kastner-Klein P, Berkowicz R, Britter R. The influence of street architecture on flow and dispersion in street canyons. Meteorology and Atmospheric Physics 2004; 87: 121-131. https://doi.org/10.1007/s00703-003-0065-4.

Kastner-Klein P, Rotach MW. Mean Flow and Turbulence Characteristics in an Urban Roughness Sublayer. Boundary-Layer Meteorology 2004; 111: 55-84. https://doi.org/10.1023/B:BOUN.0000010994.32240.b1.

Kato S, Yamaguchi Y. Analysis of urban heat-island effect using ASTER and ETM+ Data: Separation of anthropogenic heat discharge and natural heat radiation from sensible heat flux. Remote Sensing of Environment 2005; 99: 44-54. https://doi.org/10.1016/j.rse.2005.04.026.

Khalaf A. Utilization of thermal bands of Landsat 8 data and geographic information system for analysis of urban heat island in Baghdad governorate 2016. MATEC Web of Conferences 2018; 162. https://doi.org/10.1051/matecconf/201816203026.

Kleerekoper L, van Esch M, Salcedo TB. How to make a city climate-proof, addressing the urban heat island effect. Resources, Conservation and Recycling 2012; 64: 30-38. https://doi.org/10.1016/j.resconrec.2011.06.004.

Koc CB, Osmond P, Peters A. Evaluating the cooling effects of green infrastructure: A systematic review of methods, indicators and data sources. Solar Energy 2018; 166: 486-508. https://doi.org/10.1016/j.solener.2018.03.008.

Kolokotroni M, Giannitsaris I, Watkins R. The effect of the London urban heat island on building summer cooling demand and night ventilation strategies. Solar Energy 2006; 80: 383-392. https://doi.org/10.1016/j.solener.2005.03.010.

Kusaka H, Kondo H, Kikegawa Y, Kimura F. A simple single-layer urban canopy model for atmospheric models: Comparison with multi-layer and slab models. Boundary-Layer Meteorology 2001; 101: 329-358. https://doi.org/10.1023/A:1019207923078.

Kuttler W, Weber S, Schonnefeld J, Hesselschwerdt A. Urban/rural atmospheric water vapour pressure differences and urban moisture excess in Krefeld, Germany. International Journal of Climatology 2007; 27: 2005-2015. https://doi.org/ 10.1002/joc.1558.

Lampert W, Sommer U. Limnoecology: The Ecology of Lakes and Streams. New York, United States: Oxford University Press, 2007.

Lee DO. Urban—rural humidity differences in London. International Journal of Climatology 1991; 11: 577-582. https://doi.org/ 10.1002/joc.3370110509.

Lewis Jr WM. A revised classification of lakes based on mixing. Canadian Journal of Fisheries and Aquatic Sciences 1983; 40: 1779-1787.

Li C, Yu CW. Mitigation of urban heat development by cool island effect of green space and water body. Proceedings of the 8th International Symposium on Heating, Ventilation and Air Conditioning, 2014, pp. 551-561. https://doi.org/10.1007/978-3-642-39584-0_62.

Li J, Song C, Cao L, Zhu F, Meng X, Wu J. Impacts of landscape structure on surface urban heat islands: A case study of Shanghai, China. Remote Sensing of Environment 2011; 115: 3249-3263. https://doi.org/10.1016/j.rse.2011.07.008.

Liu H, Weng Q. Seasonal variations in the relationship between landscape pattern and land surface temperature in Indianapolis, USA. Environmental Monitoring and Assessment 2008; 144: 199-219. https://doi.org/10.1016/j.rse.2011.07.008.

Luo XB, Li WS. Scale effect analysis of the relationships between urban heat island and impact factors: case study in Chongqing. Journal of Applied Remote Sensing 2014; 8. https://doi.org/10.1117/1.Jrs.8.084995.

Maleki A, Kiesel K, Vuckovic M, Mahdavi A. Empirical and Computational Issues of Microclimate Simulation. Information and Communication Technology 2014; 8407: 78-85. https://doi.org/10.1007/978-3-642-55032-4_8.

Manteghi G, Limit HB, Remaz D. Water Bodies an Urban Microclimate: A Review. Modern Applied Science 2015; 9. https://doi.org/10.5539/mas.v9n6p1.

Martínez-Arroyo A, Jáuregui E. On the environmental role of urban lakes in Mexico City. Urban Ecosystems 2000; 4: 145-166. https://doi.org/10.1023/A:1011355110475.

Martins TAL, Adolphe L, Bonhomme M, Bonneaud F, Faraut S, Ginestet S, et al. Impact of Urban Cool Island measures on outdoor climate and pedestrian comfort: Simulations for a new district of Toulouse, France. Sustainable Cities and Society 2016; 26: 9-26. https://doi.org/10.1016/j.scs.2016.05.003.

Marucci D, Carpentieri M, Hayden P. On the simulation of thick non-neutral boundary layers for urban studies in a wind tunnel. International Journal of Heat and Fluid Flow 2018; 72: 37-51. https://doi.org/10.1016/j.ijheatfluidflow.2018.05.012.

Mayer H, Matzarakis A, Iziomon M. Spatio-temporal variability of moisture conditions within the Urban Canopy Layer. Theoretical and Applied Climatology 2003; 76: 165-179. https://doi.org/10.1007/s00704-003-0010-y.

Memon RA, Leung DY, Chunho L. A review on the generation, determination and mitigation of Urban Heat Island. Journal of Environmental Sciences 2008; 20: 120-128. https://doi.org/10.1016/S1001-0742(08)60019-4.

Miguet F, Groleau D. Urban bioclimatic indicators for urban planers wih the software tool Solene. SB07 Sustainable Concstruction, Materials and Practices. IOS PRESS, Lisbon, 2007, pp. 348-355.

Mirzaei PA, Haghighat F. Approaches to study Urban Heat Island – Abilities and limitations. Building and Environment 2010; 45: 2192-2201. https://doi.org/10.1016/j.buildenv.2010.04.001.

Mohan M, Kikegawa Y, Gurjar BR, Bhati S, Kolli NR. Assessment of urban heat island effect for different land use–land cover from micrometeorological measurements and remote sensing data for megacity Delhi. Theoretical and Applied Climatology 2013; 112: 647-658. https://doi.org/10.1007/s00704-012-0758-z.

Monteith JL, Unsworth MH. Principles of Environmental Physics: Academic Press, Elsevier, 2013.

Morris KI, Chan A, Ooi MC, Oozeer MY, Abakr YA, Morris KJK. Effect of vegetation and waterbody on the garden city concept: An evaluation study using a newly developed city, Putrajaya, Malaysia. Computers, Environment and Urban Systems 2016; 58: 39-51. https://doi.org/10.1016/j.compenvurbsys.2016.03.005.

Nagarajan B, Yau MK, Schuepp PH. The effects of small water bodies on the atmospheric heat and water budgets over the MacKenzie River Basin. Hydrological Processes 2004; 18: 913-938. https://doi.org/10.1002/hyp.1338.

Narita K. Effects of a river on urban thermal environment dependent on the types of on-shore building distribution. Journal of Architecture, Planning and Environmental Engineering (Transactions of AIJ) 1992; 442: 27-35 (in Japanese). https://doi.org/10.3130/aijax.442.0_27.

Nishimura N, Nomura T, Iyota H, Kimoto S. Novel water facilities for creation of comfortable urban micrometeorology. Solar Energy 1998; 64: 197-207. https://doi.org/10.1016/S0038-092X(98)00116-9.

O'Malley C, Piroozfar P, Farr ERP, Pomponi F. Urban Heat Island (UHI) mitigating strategies: A case-based comparative analysis. Sustainable Cities and Society 2015; 19: 222-235. https://doi.org/10.1016/j.scs.2015.05.009.

Oke TR. Methods in urban climatology. Applied Climatology. Zürcher Geographische Schriften 1984; 14: 19-29.

Oke TR. Boundary Layer Climates. New York: Routledge, 1987.

Oke TR. Street Design and Urban Canopy Layer Climate. Energy and Buildings 1988; 11: 103-113. https://doi.org/10.1016/0378-7788(88)90026-6.

Oke TR. The Heat Island of the Urban Boundary Layer: Characteristics, Causes and Effects. In: Cermak JE, Davenport AG, Plate EJ, Viegas DX, editors. Wind Climate in Cities. Springer Netherlands, Dordrecht, 1995, pp. 81-107. https://doi.org/10.1007/978-94-017-3686-2_5.

Oke TR, Mills G, Christen A, Voogt JA. Urban Climates: Cambridge University Press, 2017. https://doi.org/ 10.1017/9781139016476.

Oláh AB. The possibilities of decreasing the urban heat island. Applied Ecology and Environmental Research 2012; 10: 173-183. https://doi.org/10.15666/aeer/1002_173183.

Paulson CA, Pegau WS. Penetrating Shortwave Radiation*. In: Steele JH, editor. Encyclopedia of Ocean Sciences (Second Edition). Academic Press, Oxford, 2001, pp. 379-384. https://doi.org/ 10.1016/B978-012374473-9.00154-5.

Raimundo AM, Gaspar AR, Oliveira AVM, Quintela DA. Wind tunnel measurements and numerical simulations of water evaporation in forced convection airflow. International Journal of Thermal Sciences 2014; 86: 28-40. https://doi.org/10.1016/j.ijthermalsci.2014.06.026.

Raupach MR, Antonia RA, Rajagopalan S. Rough-Wall Turbulent Boundary Layers. Applied Mechanics Reviews 1991; 44: 1-25. https://doi.org/10.1115/1.3119492.

Rinner C, Hussain M. Toronto's Urban Heat Island—Exploring the Relationship between Land Use and Surface Temperature. Remote Sensing 2011; 3: 1251-1265. https://doi.org/10.3390/rs3061251.
Robinson D. Computer modelling for sustainable urban design: Physical principles, methods and applications: Routledge, 2012.
Robitu M, Inard C, Groleau D, Musy M. Energy balance study of water ponds and its influence on building energy consumption. Building Services Engineering Research and Technology 2004; 25: 171-182. https://doi.org/10.1191/0143624404bt106oa.
Robitu M, Musy M, Inard C, Groleau D. Modeling the influence of vegetation and water pond on urban microclimate. Solar Energy 2006; 80: 435-447. https://doi.org/10.1016/j.solener.2005.06.015.
Roth M, Oke TR, Emery WJ. Satellite-derived urban heat islands from three coastal cities and the utilization of such data in urban climatology. International Journal of Remote Sensing 2007; 10: 1699-1720. https://doi.org/10.1080/01431168908904002.
Saaroni H, Ziv B. The impact of a small lake on heat stress in a Mediterranean urban park: the case of Tel Aviv, Israel. Int J Biometeorol 2003; 47: 156-65. https://doi.org/10.1007/s00484-003-0161-7.
Santamouris M, Ding L, Fiorito F, Oldfield P, Osmond P, Paolini R, et al. Passive and active cooling for the outdoor built environment – Analysis and assessment of the cooling potential of mitigation technologies using performance data from 220 large scale projects. Solar Energy 2017; 154: 14-33. https://doi.org/10.1016/j.solener.2016.12.006.
Schwarz N, Schlink U, Franck U, Großmann K. Relationship of land surface and air temperatures and its implications for quantifying urban heat island indicators—An application for the city of Leipzig (Germany). Ecological Indicators 2012; 18: 693-704. https://doi.org/10.1016/j.ecolind.2012.01.001.
Shudo H, Sugiyama J, Yokoo N, Oka T. A study on temperature distribution influenced by various land uses. Energy and Buildings 1997; 26: 199-205. https://doi.org/10.1016/S0378-7788(96)01035-3.
Solcerova A, van de Ven F, Van De Giesen N. Nighttime Cooling of an Urban Pond. Frontiers in Earth Science 2019; 7: 156. https://doi.org/10.3389/feart.2019.00156.
Song K, Xenopoulos MA, Buttle JM, Marsalek J, Wagner ND, Pick FR, et al. Thermal stratification patterns in urban ponds and their relationships with vertical nutrient gradients. J Environ Manage 2013; 127: 317-23. https://doi.org/10.1016/j.jenvman.2013.05.052.
Srivastava S, Lal S, Subrahamanyam DB, Gupta S, Venkataramani S, Rajesh T. Seasonal variability in mixed layer height and its impact on trace gas distribution over a tropical urban site: Ahmedabad. Atmospheric Research 2010; 96: 79-87. https://doi.org/ 10.1016/j.atmosres.2009.11.015.
Stathopoulos T. Pedestrian level winds and outdoor human comfort. Journal of wind engineering and industrial aerodynamics 2006; 94: 769-780. https://doi.org/10.1016/j.jweia.2006.06.011.
Steeneveld GJ, Koopmans S, Heusinkveld BG, Theeuwes NE. Refreshing the role of open water surfaces on mitigating the maximum urban heat island effect. Landscape and Urban Planning 2014; 121: 92-96. https://doi.org/10.1016/j.landurbplan.2013.09.001.
Stefan HG, Horsch GM, Barko JW. A model for the estimation of convective exchange in the littoral region of a shallow lake during cooling. Hydrobiologia 1989; 174: 225-234. https://doi.org/10.1007/BF00008162.
Stull RB. An introduction to boundary layer meteorology. Vol 13: Springer Science & Business Media, 1988.
Sun R, Chen A, Chen L, Lü Y. Cooling effects of wetlands in an urban region: The case of Beijing. Ecological Indicators 2012; 20: 57-64. https://doi.org/10.1016/j.ecolind.2012.02.006.
Sun R, Chen L. How can urban water bodies be designed for climate adaptation? Landscape and Urban Planning 2012; 105: 27-33. https://doi.org/10.1016/j.landurbplan.2011.11.018.
Syafii NI, Ichinose M, Kumakura E, Jusuf SK, Chigusa K, Wong NH. Thermal environment assessment around bodies of water in urban canyons: A scale model study. Sustainable Cities and Society 2017; 34: 79-89. https://doi.org/10.1016/j.scs.2017.06.012.

Syafii NI, Ichinose M, Wong NH, Kumakura E, Jusuf SK, Chigusa K. Experimental Study on the Influence of Urban Water Body on Thermal Environment at Outdoor Scale Model. Procedia Engineering 2016; 169: 191-198. https://doi.org/10.1016/j.proeng.2016.10.023.

Taleghani M, Sailor DJ, Tenpierik M, van den Dobbelsteen A. Thermal assessment of heat mitigation strategies: The case of Portland State University, Oregon, USA. Building and Environment 2014; 73: 138-150. https://doi.org/10.1016/j.buildenv.2013.12.006.

Targino AC, Coraiola GC, Krecl P. Green or blue spaces? Assessment of the effectiveness and costs to mitigate the urban heat island in a Latin American city. Theoretical and Applied Climatology 2018. https://doi.org/10.1007/s00704-018-2534-1.

Tewari M, Chen F, Kusaka H, Miao S. Coupled WRF/Unified Noah/Urban-Canopy Modeling System. 2007.

Theeuwes NE, Solcerová A, Steeneveld GJ. Modeling the influence of open water surfaces on the summertime temperature and thermal comfort in the city. Journal of Geophysical Research: Atmospheres 2013; 118: 8881-8896. https://doi.org/10.1002/jgrd.50704.

Tombrou M, Dandou A, Helmis C, Akylas E, Angelopoulos G, Flocas H, et al. Model evaluation of the atmospheric boundary layer and mixed-layer evolution. Boundary-Layer Meteorology 2007; 124: 61-79. https://doi.org/10.1007/s10546-006-9146-5.

Tominaga Y, Sato Y, Sadohara S. CFD simulations of the effect of evaporative cooling from water bodies in a micro-scale urban environment: Validation and application studies. Sustainable Cities and Society 2015; 19: 259-270. https://doi.org/10.1016/j.scs.2015.03.011.

Tominaga Y, Stathopoulos T. CFD modeling of pollution dispersion in a street canyon: Comparison between LES and RANS. Journal of Wind Engineering and Industrial Aerodynamics 2011; 99: 340-348. https://doi.org/10.1016/j.jweia.2010.12.005.

Tomlinson CJ, Chapman L, Thornes JE, Baker CJ. Including the urban heat island in spatial heat health risk assessment strategies: a case study for Birmingham, UK. Int J Health Geogr 2011; 10: 42. https://doi.org/10.1186/1476-072X-10-42.

Toparlar Y, Blocken B, Maiheu B, van Heijst GJF. A review on the CFD analysis of urban microclimate. Renewable and Sustainable Energy Reviews 2017; 80: 1613-1640. https://doi.org/10.1016/j.rser.2017.05.248.

United Nations. World Urbanization Prospects: The 2018 Revision, 2018.

Van Buren M, Watt WE, Marsalek J, Anderson B. Thermal enhancement of stormwater runoff by paved surfaces. Water Research 2000; 34: 1359-1371. https://doi.org/10.1016/S0043-1354(99)00244-4.

van Hooff T, Blocken B. Coupled urban wind flow and indoor natural ventilation modelling on a high-resolution grid: A case study for the Amsterdam ArenA stadium. Environmental Modelling & Software 2010a; 25: 51-65. https://doi.org/10.1016/j.envsoft.2009.07.008.

van Hooff T, Blocken B. On the effect of wind direction and urban surroundings on natural ventilation of a large semi-enclosed stadium. Computers & Fluids 2010b; 39: 1146–1155. https://doi.org/10.1016/j.compfluid.2010.02.004.

Völker S, Baumeister H, Claßen T, Hornberg C, Kistemann T. Evidence for the temperature-mitigating capacity of urban blue space – a health geographic perspective. Erdkunde 2013; 67: 355-371. https://doi.org/10.3112/erdkunde.2013.04.05.

Wang K, Wang J, Wang P, Sparrow M, Yang J, Chen H. Influences of urbanization on surface characteristics as derived from the Moderate-Resolution Imaging Spectroradiometer: A case study for the Beijing metropolitan area. Journal of Geophysical Research-Atmospheres 2007; 112. https://doi.org/10.1029/2006JD007997.

Webb BW, Hannah DM, Moore RD, Brown LE, Nobilis F. Recent advances in stream and river temperature research. Hydrological Processes 2008; 22: 902-918. https://doi.org/10.1002/hyp.6994.

Webb BW, Zhang Y. Spatial and seasonal variability in the components of the river heat budget. Hydrological Processes 1997; 11: 79-101. https://doi.org/10.1002/(Sici)1099-1085(199701)11:1<79::Aid-Hyp404>3.3.Co;2-E.

Weng Q, Lu D, Schubring J. Estimation of land surface temperature–vegetation abundance relationship for urban heat island studies. Remote Sensing of Environment 2004; 89: 467-483. https://doi.org/10.1016/j.rse.2003.11.005.

Xu J, Wei Q, Huang X, Zhu X, Li G. Evaluation of human thermal comfort near urban waterbody during summer. Building and Environment 2010; 45: 1072-1080. https://doi.org/10.1016/j.buildenv.2009.10.025.

Xue Z, Hou G, Zhang Z, Lyu X, Jiang M, Zou Y, et al. Quantifying the cooling-effects of urban and peri-urban wetlands using remote sensing data: Case study of cities of Northeast China. Landscape and Urban Planning 2019; 182: 92-100. https://doi.org/10.1016/j.landurbplan.2018.10.015.

Yang X, Peng LL, Chen Y, Yao L, Wang Q. Air humidity characteristics of local climate zones: A three-year observational study in Nanjing. Building and Environment 2020; 171: 106661. https://doi.org/ 10.1016/j.buildenv.2020.106661.

Yang X, Zhao L. Diurnal Thermal Behavior of Pavements, Vegetation, and Water Pond in a Hot-Humid City. Buildings 2016; 6: 2. https://doi.org/10.3390/buildings6010002.

Zhao TF, Fong KF. Characterization of different heat mitigation strategies in landscape to fight against heat island and improve thermal comfort in hot-humid climate (Part I): Measurement and modelling. Sustainable Cities and Society 2017b; 32: 523-531. https://doi.org/10.1016/j.scs.2017.03.025.

Zhao TF, Fong KF. Characterization of different heat mitigation strategies in landscape to fight against heat island and improve thermal comfort in hot-humid climate (Part II): Evaluation and characterization. Sustainable Cities and Society 2017a; 35: 841-850. https://doi.org/10.1016/j.scs.2017.05.006.

Žuvela-Aloise M, Koch R, Buchholz S, Früh B. Modelling the potential of green and blue infrastructure to reduce urban heat load in the city of Vienna. Climatic Change 2016; 135: 425-438. https://doi.org/10.1007/s10584-016-1596-2.

Table 3: Comparative analysis of observational studies.

Reviewed study	Type – climate	Method	Waterbody characteristics	Season – part of the day	Weather conditions	Key findings
Ishii et al. (1991)	Pond – Fukuoka, Japan (Cfa)	Field measurements	Size: 127,000 m² Shape: Elongated (N-S)	Summer (August) – 7:00 – 19:00	Air Temp.: 28.7 °C Wind speed: 7.7 - 8 m/s Wind direction: northerly	Max 3 °C cooling effect during afternoon hours (12:00 – 15:00)
Nishimura et al. (1998)	Pond – Osaka, Japan (Cfa*)	Field measurements & wind tunnel tests	Depth: 0.2 m Surrounding environment: Urban Shape: Elongated (N-S)	Summer (July) – 24h	Air Temp.: 35 °C Wind speed: 2.5 m/s Wind direction: west-north-westerly	Pond alone: Reduced air temperatures on leeward side by up to 2 °C between 14:00 and 15:00
Saaroni & Ziv (2003)	Pond – Tel Aviv, Israel (Csa)	Field measurements	Size: 40,000 m² Surrounding environment: Open, grass-covered area Shape: Elongated (SW-NE)	May and June (two days – dry/humid) – 7:30 – 19:00	Dry and hot: 2 – 10 m/s Sultry: 2 – 8 m/s Wind direction: west-north-westerly	*Lake effect*: up to 1.6 °C temperature drop and 6% increase of humidity at midday Warming effect during evening hours Even small waterbodies can have a relieving effect on humans
Huang et al. (2008a,b)	Urban water areas – Nanjing, China (Cfa)	Field measurements	Size: 3.7 km²	Hot period (July - September) – 24h	Mean air temp.: 21 – 30.5 °C Mean RH: 68 – 82% Mean wind speed: 1 – 4.3 m/s	During the night (22:00 – 4:00) water areas are warmer by 0.3-0.7 °C than concrete surfaces Max cooling effect of 3.5 °C at 16:00 (wind speed: 1.3 m/s, RH: 77%, cloud cover: 3.1)
Chen et al. (2009)	Artificial lake – Guangzhou, China(Cfa)	Field measurements	Surrounding environment: Urban Shape: ~circular	Summer (July) – 5 days (10:00 – 17:00)	Air temp.: 28-36 °C RH: 45-85% Wind Direction.: South or SE 0 – 3 m/s Air temp.> 35 °C	Average air temperature reduction of 1.3 °C at measurement points along the lake compared to points far away of it Maximum cooling effect is 2.2 °C at noon
Xu et al. (2010)	Lake, Shanghai, China (Cfa)	Field measurements against the Heat index method	Size: 87,000 m² Surrounding environment: Green space & concrete paved roads Water temperature: 32 °C Evaporation rate: 0.0004872 m/h	Summer (August, July) – Day (10:00 – 16:00)		Heat index method has been proved suitable for thermal comfort evaluation in littoral zones Effective improvement of thermal comfort near waterbody (positive relationship with surface area) Most efficient at 10-20 m from lake's edge. (at 15 m distance a cooling effect of almost 3 °C was found) Synergistic cooling
Heusinkveld et al. (2014)	Urban waterbodies (a river is included) – Rotterdam, Netherlands (Cfb)	Mobile measurements	Local-scale waterbodies Different shapes	Summer (August) – Day (11:30 – 13:40) & night (20:10 – 22:10)	Diurnal temperature variation <2 °C Wind direction: varied between NE-ESE	Night-time UHI of 7 °C - Daytime UHI of 1.2 °C Waterbodies can have a negative thermal effect during the night Up to 4 °C difference in air temperature at midday
Li & Yu (2014)	Three lakes (and six parks) – Chongqing, China (Cfa)	Field measurements	Size: 8,800 - 17,600 - 69,600 m²	Summer (July – August) – Day (9:00 – 17:00)	Calm days	Maximum cooling effect of lakes was 2.9 °C, while that of parks was 3.6 °C The less the landscape shape index or the rounder the shape, the better the cooling effects of parks and lakes

Steeneveld et al. (2014)	Urban waterbodies Netherlands (Cfb)	Hobby meteorological observations	Surrounding environment: Urban, limited green space Mean WB coverage: ~4%	Different times throughout the year	N/A	UHI is dependent on open water fraction Increase of the 95th percentile of the daily maximum UHI
Yang & Zhao (2015)	Guangzhou, China (Cfa)	Field measurements	Depth: ~2 m	Summer (July) – 24h	Air Temp.: 27.6-36.2 °C RH: 44-84% Wind speed: 1.1 m/s	Daytime (8:00 – 19:00): Pond was 2.2 °C cooler than air temperature Night-time (20:00 – 7:00): Pond was warmer by 0.8 °C Maximum air temperature reduction of 1.5 °C
Syafii et al. (2016)	Pond – Saitama, Japan (Cfa)	Down-scaled experimental model	Dimensions: 1.5 m wide, 6 m long Depth: 0.1 m	Summer – Two months – 24h Day: 6:00 - 18:00 Night: 18:00 - 6:00	N/A	Maximum cooling effect of 2.6 °C Warming effect up to 0.7 °C during the night
Syafii et al. (2017)	Ponds – Saitama, Japan (Cfa)	Down-scaled experimental model	Small pond: 1.5m × 0.5 m Big pond: 1.5 × 6 m Depth: 0.15 m	Summer – 24h Day: 6:00 - 18:00 Night: 18:00 - 6:00	N/A	The larger the pond is the higher the cooling effect in the nearby area Ponds parallel to prevailing winds are more effective. (on average 1.6 °C cooling effect) Cooling effect of small and big ponds was up to 0.7 °C and 1.25 °C, respectively
Targino et al. (2018)	Lake, Londrina, Brazil (Cfa)	Field measurements	Area: 168,100 m² Avg. depth: 2 m Shape: elongated (NW-SE)	Late Autumn (May – June) – Several days	Mean daily air temperature 15.3 - 21.2 °C	The vegetated area always cooler than the lake On 30th May, the lake's cooling effect was 1.8 °C at 13:00
Solcerova et al. (2019)	Urban pond, Delft, The Netherlands (Cfb)	Field measurements	Depth: ~70 cm Area: 3,627 m²	Summer (July 12th – August 7th) – Night: 23:00 – 5:00)	Air temp.: Daytime: 15-34 °C, Night-time: 15-27 °C Mean wind speed: 0.3 m/s	On an everage summer night, from a total of 2.7 MJ/m² 11% was realesed as sensible heat, 43% as longwave radiation, 39% as latent heat and the rest was transferred to the bottom of the lake

*Climates are categorised according to the Köppen–Geiger climate classification system – full abbreviation description can be found in Table 6.

Table 4: Comparative analysis of selected remote sensing studies.

Reviewed study	Type – climate	Waterbody characteristics	Season – part of the day	Weather conditions	Key findings
Cao et al. (2010)	PCI intensity of 92 parks – Nagoya, Japan (Cfa*)	Parks size: 1,000 – 419,000 m²	Three days in spring, summer & autumn – morning	N/A	Waterbody didn't affect PCI formation Irregular and belt-shaped parks lead to less cooling effects
Rinner & Hussain (2011)	Water areas – Toronto, Canada (Dfb)	N/A	September – morning (10:00)	26.3 °C, 46%, 2 m/s Wind dir.: West	Waterbodies are the main cooling element
Sun et al. (2012)	Waterbodies – Beijing, China (Dwa)	Mean size: 9.76 km² Mean LSI: 7.25 Mean temperature: 28.33 °C	Summer – morning	Mean temp. of green space: 28.43 °C Mean temp. of built-up area: 31.82 °C	DIST is significantly important Cooling effect of wetland decreases with WA[1] UCI intensity is highly correlated with shape Mean cooling intensity of 3.15 °C
Sun & Chen (2012)	UCI intensity & efficiency of 197 waterbodies – Beijing, China (Dwa)	Total size: 90,000 m² Mean temperature: 29.49 °C Average area: 45,100 m²	Summer – morning	Mean temp. of green space: 30.07 °C Mean temp. of built-up area: 32.86 °C	UCI intensity increases with PB[1] and WA UCI intensity decreases with LSI[1] and location DIST[1] UCI efficiency increases with PB UCI efficiency decreases with LSI, DIST and WA Maximum cooling intensity of 2.2 °C/hm
Oláh (2012)	Budapest, Hungary (Dfb)	N/A	Spring	N/A	Green and blue spaces can mitigate UHI phenomenon Cooling effect up to 10 °C
Schwarz et al. (2012)	Leipzig, Germany (Cfb)	N/A	Autumn – morning & evening	Mean air temp.: 14.7 °C Mean RH: 78.1% Avg. wind speed: 2 m/s	Cooling effect of 4 °C and 1 °C in the morning and evening
Hou et al. (2012)	Beijing, China (Dwa)	N/A	Spring – Day	N/A	Waterbodies significantly affect near-surface temperatures at a distance less than 300 m
Chun & Guhathakurta (2016)	Atlanta, USA (Cfa)	N/A	April (night-time: 03:43) & August (daytime: 16:20)	Clear sky	Waterbodies decrease LST during the day but increase LST at night
Du et al. (2016)	21 waterbodies – Shanghai, China (Cfa)	N/A	Summer	N/A	Mean cooling potential of 3.32 °C Cooling decreases with shape and the proportion of impervious materials Cooling increases with the proportion of vegetation
Chowdhury et al. (2017)	Pune, India (Aw)	72,000 m² - 626,000 m²	March (daytime)	N/A	Lake's cooling potential of 8.1 °C
Cai et al. (2018)	Chongqing, China (Cfa)	N/A	Summer	N/A	Waterbodies are strongly related to urban form and LST at a distance less than 500 m
Khalaf (2018)	Baghdad, Iraq (Bwh)	N/A	August (10:33) – two days	N/A	Blue spaces were found 6 °C cooler than the surrounding built-up area

Dai et al. (2019)	Beijing's Olympic Area, China (Dwa)	WB coverage: ~2.4%	May (10:52)	Clear sky	Waterbodies were found to have the lowest surface temperatures
He et al. (2019)	Shenyang, China (Dwa)	WB coverage: 3.7%	July (10:27)	Air Temp.: 31.4 °C Cloud cover: 0.04% RH: 36.5% Wind speed: 1.55 m/s	Waterbodies were found to be the coolest urban element providing up to 10 °C cooling effect Waterbodies' cooling potential is decreasing with increasing air temperatures
Xue et al. (2019)	Changchun & Jilin, China (Dwa)	21 urban wetlands & 3 green parks	July (10:21)	Air temp.: min: 19.4 °C, max: 32.4 °C Wind speed: ~1.7 m/s	Mean cooling potential of 2.74 °C The cooling potential of rivers is higher than that of other waterbodies and green spaces Waterbodies of more complex shape lead to an increased cooling effect
Wu & Zhang (2019)	Suzhou, China (Cfa)	WB coverage (Suzhou Bay): 32.34%	April (10:30)	N/A	Maximum cooling effect of 3.02 °C The cooling distance can reach up to 800 m

*Climates are categorised according to the Köppen–Geiger climate classification system – full abbreviation description can be found in **Error! Reference source not found.**.

[1]WA: Waterbody area, PB: Built-up proportion, LSI: Land Shape Index, DIST: Distance from the city

Table 5: Comparative analysis of simulation studies.

Reviewed study	Case Study – Climate	Target parameter	Numerical tool – Validation	Domain – Waterbody characteristics	Season – Period of analysis	Set-up parameters.	Key Findings
Nagarajan et al. (2004)	Mackenzie River Basin, Canada (Dfc)[1]	AT, SHF, LHF	Canadian compressible community (MC2) model (mesoscale) – Aircraft measurements	WB coverage: 10% Water temp.: 11-15 °C WB shape: assumed circular	Warm season (June) – 19:00-24:00	Wind direction: EW & NS	Up to 9% (82%) decrease (increase) of mean surface sensible (latent) heat flux Apparent warming up to 150 m height Cooling occurs above 150 m
Robitu et al. (2004)	Ponds & building energy consumption – Bucharest, Romania (Cfa)	AT	Coupling of SOLENE and ANSYS Fluent CFD tool	4 m length pond inside a street canyon Depth: 0.5 m Shape: square	Summer (June) – Day	Air temp.: 301K (~28 °C) Wind speed: 5 m/s	1 °C air temperature decrease at 30 m distance & 1 m height (at 15:00)
Robitu et al. (2006)	Ponds & trees – Nantes, France (Cfb)	MRT, PMV	Coupling of SOLENE and ANSYS Fluent CFD tool	Depth: 0.5 m Concrete layer: 0.2 m WB shape: elongated	Summer (July) – 8:00-16:00	Air temp.: 21-32 °C Wind: 2 m/s (10 m) Wind direction: southerly RH: 55%	PMV (at 14:00): • 3.4 without the water pond • 0.54 (neutral comfort zone) with the pond
Yamaoka et al. (2008)	Street canyon – Osaka, Japan (Cfa)	AT, MRT, SET	CFD numerical code	Two water streams along the two walkways of the street canyon WB dimensions: 564 x 3 m Water temp.: 30 °C WB shape: elongated	Summer (August) – 10:00-15:00	Air temp: 36.5 °C Wind speed: 1.3 m/s MRT: 34.2 SET: 32.2	Air temperature decrease by up to 1.2 °C MRT decrease by up to 0.4 °C SET decrease by up to 0.5 °C
Theeuwes et al. (2013)	Lakes on an idealized round-shaped city (Cfb)	AT	WRF (meteorological model) /Noah/UCM (mesoscale)	Diameter: 50 km (2,000 cells) High-density built-up area Water temp.: 10, 15, 20 °C WB coverage: 5, 10, 15% WB shape: square and circular	Spring (May) – 84h simulation (24h spin-up)	Air temp.: 18-25 °C Wind: 2.5 – 5 m/s (10 m) Wind direction: south-easterly	Modelled UHI: ~1 °C between 10:00-18:00, ~6 °C between 23:00-2:00 Water temp.: 15 °C: Max cooling of 1.2-1.8 °C at 10:00 Max warming of 0.7-1 °C at 6:00 Larger lakes present higher cooling effect close to their edges and in downwind areas Equally distributed smaller lakes influence a larger area with a smaller temperature effect
Taleghani et al. (2014)	Portland, USA (Csb)	AT	ENVI-met (microscale) – Field measurements	No evidence of the simulation set-up WB shape: square	Summer (July) – 24h	Wind direction: NW	Max cooling effect of 1.1 °C (between 15:00-16:00)
Müller et al. (2013)	Oberhausen, Germany (Cfb)	PET	ENVI-met (microscale) – Field measurements	Domain: 460×460 m WB size: (i) 4,000 m², (ii) 10,000 m² WB shape: elongated and square	Summer (July)– 44h (19h spin-up)	Air Temp.: 22.7-35.2 °C Wind speed: 1-3 m/s Wind direction: east-north-easterly	(i): maximum reduction of PET by 2.54 °C (ii): maximum reduction of PET by 14.90 °C Wind speed is the most important parameter in improving thermal comfort. Even slightly increased velocities can lead to significant reduce of PET
Amor et al. (2015)	Sétif, Algeria (Csa)	AT, PMV	ENVI-met (microscale) – Field measurements	Domain: 70 m x 80 m WB size: (i) 214 m², (ii) 770 m² WB coverage: (i) 3.7%, (ii) 34%	Summer (August) – 6:00-20:00	Wind: 0.4-0.5 m/s	(i) Max cooling effect of 0.32 °C at 6:00, min cooling of 0.08 °C at13:00 (ii) Mean cooling effect of 0.009 °C
Tominaga et al. (2015)	Pond – Hadano City, Japan (Cfa)	AT	ANSYS Fluent (microscale) – Field measurements	Body-fitted technique Depth: 0.003 m Water temp.: 23.1 & 22.1 °C WB shape: elongated	Summer (August) – Day (results only for 15:00)	Air Temp.: 33.7 & 32.8 °C Wind: 3.8 & 3.1 m/s Wind direction: WSW & WNW RH: 60 & 64%	Maximum temperature decrease of 2 °C at the pedestrian level Downwind cooling effect over 100 m Simulation of evaporation
O'Malley et al. (2015)	Ponds – West Kensington, London, UK (Cfb)	AT	ENVI-met (microscale) – Field measurements	N/A	10:00-20:00	N/A	The presence of waterbodies does not mitigate UHI (Maximum cooling potential of 0.4 °C) All microclimate effects should be included if one wants to study the UHI with precision

Morris et al. (2016)	Lakes and wetlands – Putrajaya, Malaysia (Af)	AT	WRF/Noah/UCM (mesoscale) – Field measurements	WB coverage: 12% Dispersed urban form, low density	September – 66h simulation (16h spin-up)	N/A	0.4 °C average reduction of (2 m) air temperature (11:00 – 16:00) 0.1 °C average warming effect during night-time and early morning (1:00 – 10:00)
Martins et al. (2016)	Pool, ponds & fountains – Toulouse, France (Cfb)	AT, PET	ENVI-met (microscale)	Domain: 230x230x26	Summer (June) – 24h (results for 12:00 & 24:00 only)	Wind speed: 3.6 m/s (at 10 m) Wind direction: Southerly	Max cooling at 12:00: 6 °C Max cooling at 24:00: 2 °C No significant improvement of thermal comfort
Žuvela-Aloise et al. (2016)	Vienna, Austria (Cfb)	AT	MUKLIMO_3	Domain: 60x60 (100 m horizontal grid spacing) WB size: 250,000 m² Water temp.: 18 & 23 °C WB coverage: 4.6%	Summer – 24h	T = 25 °C, R = 42% Wind: 0.7 & 4 m/s Dense and low-dense built-up area	Maximum cooling effect of 1.75 °C Water temp: 18 °C: Cooling at 14:00, 22:00 & 4:00 Water temp: 23 °C: Cooling at 14:00 & 22:00; Warming at 4:00
Song et al. (2016)	Harbin City, China (Dwa)	AT, VP	Fluent 6.3 – Wind tunnel experiment	Domain: 3200 x 2000 x 305 mm Water temp.: 27.2 °C	N/A	Air Temp.: 31.2 °C Wind speed (10m): 2.8 m/s	Increased building floor area leads to decreased transport of water vapour due to reduced wind velocities The increased building floor area can increase or decrease the air temperature depending on the wind and shading effects
Jin et al. (2017)	Ponds – Harbin City, China (Dwa)	AT, RH	ENVI-met (microscale) – Field measurements	Simulation: Centralized and dispersed waterbodies in a residential urban district WB coverage: 6%	Field measurements: Summer (July) – Day (9:30 – 14:30) Simulation: Summer (July) – Day (9:00 – 16:00)	Simulation: Wind: SW, 2 m/s Air Temp.: 21 °C RH: 75.6%	Centralized ponds should be placed in against the dominant wind direction More dispersed waterbodies can have a more uniform cooling effect
Zhao & Fong (2017 – Part I & II)	Waterbodies in idealised model – Hong Kong (Cfa)	AT, PET	ENVI-met (microscale)	Building coverage: 44% Blue space in different area coverage ratios (8 – 56%) WB shape: square	Summer (August) – Day (15:00)	Wind: 1.24 m/s (at 10 m) Wind direction: Easterly	Cooling effect of 0.7 – 1.5 °C If R_{HMS} > 34%: Positive impact (0.7 °C) If R_{HMS} < 34%: Negative impact (increased RH will lead to heat stress)
Abbasi et al. (2018)	Lake Binaba, Ghana (Aw)	AT, WS	OpenFOAM – Field measurements	WB size: 31,000 m² Avg. depth: 1.1 m Max. depth: 4 m Water temp.: 24-32.5 °C	Field measurements: November 23 – December 23, 2012 Simulation: Duration: 4 days	Air temp.: 18-40 °C Wind: SW, max. speed 4.5 m/s Domain: 3,500 m x 1,850 m x 500 m Cell size: 10 m x 10 m x 0.1 m Cell refinement near water surface in z direction: 0.01-0.02 m:	Unstable atmosphere: Sharp changes in velocity profile – no changes in temperature profile Stable atmosphere: Sharp changes (increase or decrease) in temperature profile – no clear pattern for velocity profile

[1] Climates are categorised according to the Köppen–Geiger climate classification system – full abbreviation description can be found in **Error! Reference source not found.**.

Abbreviations: AT, Air temperature (°C); LHF, latent heat flux (W/m²); MRT, mean radiant temperature (°C); PET, physiological equivalent temperature (K); PMV, predicted mean vote (-); RH, relative humidity (%); SET, standard effective temperature (°C); SHF, sensible heat flux (W/m²); WV, wind velocity (m/s); VP, vapour pressure ratio (-).

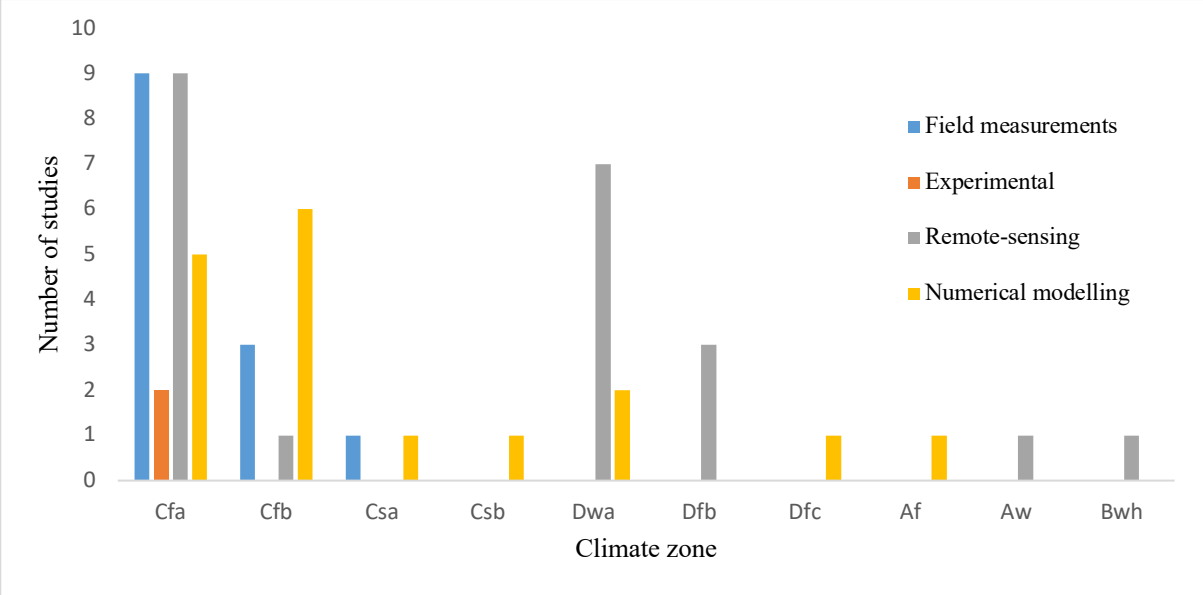

Figure 7: Distribution of reviewed studies per climate zones (full abbreviation description can be found in Table 6).

Table 6: All different climates found in the reviewed studies under the Köppen–Geiger climate classification.

Climate	Name	Characteristics
Af	Tropical rainforest	• Average monthly temperature ≥18 °C • Average monthly precipitation ≥60 mm
Aw	Tropical savannah	• Average monthly temperature ≥18 °C • Driest month's precipitation ≤60 mm
BWh	Hot desert climate	• Low-latitude climate • Average annual temperature ≥18 °C • Excess of evaporation over precipitation
Cfa	Humid subtropical	• Average coldest month's temperature >0 °C • Negligible precipitation difference between seasons • At least one month's mean temperature >22 °C • No dry months in the summer
Cfb	Temperate oceanic	• Average coldest month's temperature >0 °C • Negligible precipitation difference between seasons • Every month's mean temperature <22 °C
Csa	Hot-summer Mediterranean	• Average coldest month's temperature >0 °C • At least one month's mean temperature >22 °C • At least 3x as much precipitation in the wettest month of winter as in the driest month of summer
Csb	Warm-summer Mediterranean	• Average coldest month's temperature >0 °C • Every month's mean temperature <22 °C • At least 3x as much precipitation in the wettest month of winter as in the driest month of summer
Dfb	Warm-summer humid continental	• Average coldest month's temperature <0 °C • Negligible precipitation difference between seasons • Every month's mean temperature <22 °C
Dfc	Subarctic	• Average coldest month's temperature <0 °C • Up to 3 months averaging >10 °C • Negligible precipitation difference between seasons
Dwa	Monsoon-influenced hot-summer humid continental	• Average coldest month's temperature <0 °C • At least 10x as much rain in the wettest month of summer as in the driest month of winter